UC Berkeley
UC Berkeley Electronic Theses and Dissertations

Title

Innate immune responses to soluble factors from Pseudomonas aeruginosa

Permalink

https://escholarship.org/uc/item/0s34q7bv

Author

Grabiner, Mark Aaron

Publication Date

2013

Peer reviewed|Thesis/dissertation

Innate immune responses to soluble factors from *Pseudomonas aeruginosa*

by

Mark Aaron Grabiner

A dissertation submitted in partial satisfaction of the requirements for the degree of

Doctor of Philosophy

in

Molecular and Cell Biology

in the

Graduate Division

of the

University of California, Berkeley

Committee in charge:

Professor Terry Machen, Chair

Professor Russell Vance

Professor Ehud Isacoff

Professor Kathleen Ryan

Fall 2013

Abstract

Innate immune responses to soluble factors from *Pseudomonas aeruginosa*

by

Mark Aaron Grabiner

Doctor of Philosophy in Molecular and Cell Biology

University of California, Berkeley

Professor Terry Machen, Chair

Pseudomonas aeruginosa are gram-negative bacteria that colonize the human airway. They are of great clinical importance, especially for patients with the genetic disorder Cystic Fibrosis, a disease characterized by persistent infection and hyper-inflammation in the airways (Hoiby *et al.*, 1977). The innate immune response to *P. aeruginosa* in airway cells consists of fluid secretion driven by the Cystic Fibrosis Transmembrane conductance Regulator (CFTR) and the release of inflammatory cytokines for the recruitment of phagocytes. The present work addresses the role of two secreted products from *P. aeruginosa* and their effects on these processes. Flagellin, the protein monomer of the *P. aeruginosa* flagellum, has been previously shown to induce cytokine secretion through Toll-Like Receptor 5 (TLR5) (Zhang *et al.*, 2005) and to activate CFTR-mediated secretion through an unknown mechanism (Illek *et al.*, 2008). In the present study I attempted to discover the signaling pathway mediating CFTR secretion from flagellin. Though this work did not yield a definitive pathway, many possibilities were explored and the response to flagellin was better characterized than in previous work. In addition to my study of flagellin, I also studied the effects of a *P. aeruginosa* quorum-sensing signaling molecule, N-(3-Oxododecanoyl)-L-homoserine lactone (HSL-C12), on inflammatory signaling in mammalian cells. Previous work has characterized the response to HSL-C12 as either pro- or anti-inflammatory depending on the system used and the measurements taken (Telford *et al.*, 1998, Smith *et al.*, 2001, Smith *et al.*, 2002, Kravchenko *et al.*, 2006, Jahoor *et al.*, 2008, Kravchenko *et al.*, 2008). In my study I utilized both gene expression and cytokine secretion measurements to determine that HSL-C12 has anti-inflammatory characteristics in short treatments but pro-inflammatory characteristics in longer treatments and that both of these phenotypes stem from an inhibition of host protein synthesis. Together with what is already known about *P. aeruginosa* infection, my data helps to paint a picture of how secreted factors affect the course of infection and inflammatory response to *P. aeruginosa* in the human airway.

TABLE OF CONTENTS

LIST OF FIGURES

Chapter 1

Chapter 2

ABBREVIATIONS USED

AC	Adenylate Cyclase
AP	Apical
ASL	Airway Surface Liquid
ATP	Adenosine Triphosphate
BAPTA	1,2-bis(o-aminophenoxy)ethane-N,N,N',N'-tetraacetic acid
BL	Basolateral
bpV	Potassium Bisperoxo(1,10-phenanthroline)oxovanadate (V)
Ca^{2+}	Ionic Calcium
CaCC	Ca^{2+}-activated Chloride Channels
cAMP	Cyclic Adenosine Monophosphate
CF	Cystic Fibrosis
CFTR	Cystic Fibrosis Transmembrane conductance Regulator
cGKII	cGMP-dependent Kinase II
Cl^-	Ionic Chloride
DMEM	Dulbecco's Modified Eagles Medium
eI-F2α	Eukaryotic Initiation Factor 2 alpha
ELISA	Enzyme Linked ImmunoSorbent Assay
GCN2	General Control Nonrepressed 2
GFP	Green Fluorescent Protein
GPCR	G-Protein Coupled Receptor
HSL-C12	N-(3-Oxododecanoyl)-L-homoserine lactone
IBMX	Isobutylmethylxanthine
I_{Cl}	Transepithelial chloride current
IκB	Inhibitor of nuclear factor κB
IL-1β	Interleukin 1 beta
IL-8	Interleukin 8
IP_3R	Inositol trisphosphate receptor
KC	Keratinocyte-derived Chemokine
MEF	Mouse Embryonic Fibroblasts
NBD	Nucleotide Binding Domain
NF-κB	Nuclear Factor κB
NKCC	Na-K-Cl Cotransporter
PBS	Phosphate Buffered Saline
PBSA	Phosphate Buffered Saline with Bovine Serum Albumin
PBST	Phosphate Buffered Saline with Tween-20
PDE	Phosphodiesterase
PERK	Eukaryotic translation initiation factor 2-alpha kinase 3
PI3K	Phosphatidylinositide 3-kinase
PKA	Protein Kinase A
PKC	Protein Kinase C
PLC	Phospholipase C
PM	Plasma Membrane
PTEN	Phosphatase and Tensin homolog
qPCR	Quantitative Polymerase Chain Reaction
RIPA	Radioimmunoprecipitation Assay Buffer

SDS-PAGE   SDS Polyacrylamide-Gel Electrophoresis
SERCA   Sarco/Endoplasmic Reticulum Ca^{2+}-ATPase
SOCE   Store-Operate Calcium Entry
SOcAMP   Store-Operate cAMP
STIM1   Stromal Interaction Molecule 1
TNFα   Tumor Necrosis Factor α
TLR5   Toll-Like Receptor 5
WT   Wild Type
XesC   Xestospongin C

ACKNOWLEDGEMENTS

Chapter 1

CFTR currents induced by exposure to *Pseudomonas aeruginosa* flagellin

INTRODUCTION

The flagellin protein from *P. aeruginosa* induces an increase in CFTR currents in airway epithelial cells, through a mechanism that has not yet been fully elucidated (Illek *et al.*, 2008). Flagellin is the bacterial protein monomer that forms the bacterial flagellum. Flagellin peptides are trafficked through both bacterial membranes via an export machinery similar to the type-three secretion system. The peptides traverse the length of the nascent flagellum within the hollow interior and are then positioned at the growing end with the help of a cap protein. Flagellin contains an epitope that is recognized by the innate immune receptor toll-like receptor 5 (TLR5) (Hayashi *et al.*, 2001). The epitope is buried in the intact flagellum but is accessible on free flagellin (Smith *et al.*, 2003). *P. aeruginosa* flagellin induces cytokine production in airway epithelial cells through TLR5 signaling (Zhang *et al.*, 2005). TLR5 activation, through the mediator MyD88 and downstream targets, causes the phosphorylation and degradation of IκB, the inhibitory subunit of the cytosolic NF-κB complex (Choi *et al.*, 2010). The transcription factor p65 is then freed to enter the nucleus and drive inflammatory gene transcription.

CFTR is a chloride/bicarbonate anion channel in the ABC protein transporter family that is found prominently in many epithelia, but also in other cells like leucocytes, smooth muscle and neurons, in the human body (Gadsby *et al.*, 2006). Its role as an ion channel rather than a transporter makes it unique among ABC proteins. CFTR possesses the classic ABC family structure with two transmembrane domains, each with six membrane-spanning helices, along with two nucleotide binding domains (NBDs) and a unique R domain. The R domain includes multiple phosphorylation sites for both protein kinase A (PKA), the kinase activated by cyclic adenosine monophosphate (cAMP), and protein kinase C (PKC), the kinase activated by Ca^{2+} and diacylglycerol (Cheng *et al.*, 1991, Bear *et al.*, 1992, Liedtke *et al.*, 1998). Activation of CFTR by cGMP-dependent kinase II (cGKII) has also been observed in fibroblasts, rat intestinal cells, and human Clara airway cells (French *et al.*, 1995, Kulaksiz *et al.*, 2002). Phosphorylation of the R domain by PKA allows the NBDs to bind two ATP molecules and dimerize in a head-to-tail fashion, opening the channel (Gadsby *et al.*, 1999). It has also been proposed that phosphorylation of PKC sites is required for actions of PKA or that phosphorylation of PKC sites facilitates the phosphorylation of PKA sites. Membrane-bound protein phosphatases of the PP2C family constitutively dephosphorylate CFTR, thereby requiring active PKA to open CFTR (Hanrahan *et al.*, 2003). Excised patches of CFTR with no cAMP or PKA lose conductance in about 10 seconds (Becq *et al.*, 1994). Overall, it is clear that cAMP, acting through PKA, is central to the regulation of CFTR, while Ca^{2+} and diacylglycerol, acting through PKC, may play modulatory roles. cGMP acting through cGKII may also play a role in CFTR regulation, though this has not been established in the cell types used for this study.

cAMP is produced by a group of enzymes called adenylate cyclases (ACs) and is degraded by phosphodiesterases (PDEs) (Hanoune *et al.*, 2001). Previous unpublished work in the Machen lab had shown that cAMP is likely involved in flagellin-induced CFTR currents: the PKA antagonist RpBrcAMPS prevented flagellin-induced chloride currents while the phosphodiesterase blocker isobutylmethylxanthine (IBMX) enhanced flagellin-stimulated currents. It had also been reported that flagellin stimulated release of ER calcium and increases in cytosolic calcium in some human airway epithelial cell lines (Adamo *et al.*, 2004, West *et al.*, 2005), though other airway lines showed no increases in cytosolic Ca^{2+} in response to flagellin (Fu *et al.*, 2007). ACs, which produce cAMP, have been shown to be regulated primarily by G

proteins, but also by Ca^{2+} and STIM1, a transmembrane ER calcium sensor responsible for regulating store-operated calcium entry (SOCE) (Hanoune *et al.*, 2001, Lefkimmiatis *et al.*, 2009). The ER lumenal side of STIM1 contains a calcium-binding EF hand, and the cytosolic side contains protein interaction domains known to directly gate ORAI, the plasma membrane (PM) calcium channel associated with SOCE (Ong *et al.*, 2007). Calcium levels are maintained in the ER through the action of the sarco/endoplasmic reticulum Ca^{2+}-ATPase (SERCA) which pumps cytosolic calcium into the ER (Christensen *et al.*, 1993). Calcium is released from the ER primarily through the inositol trisphosphate receptor (IP_3R), which is opened by the ligand inositol trisphosphate produced by the enzyme phospholipase C (PLC). When calcium levels drop in the ER, STIM1 forms multimers that translocate to portions of the ER adjacent to the PM; STIM1 then activates ORAI and lets in a flood of extracellular calcium. It has been proposed that calcium release from the ER can also activate cAMP production by ACs in a STIM1-dependent manner in the absence of extracellular calcium (Lefkimmiatis *et al.*, 2009). These data suggested that STIM1 and AC interact directly. This signaling pathway was dubbed store-operated cAMP (SOcAMP). Because SOcAMP requires the release of ER calcium, which has been observed in response to flagellin by the Machen lab, but not necessarily an observable increase in cytosolic calcium, which has not been observed by the Machen lab, I decided to examine the role of calcium signaling, STIM1, and cAMP production in flagellin-induced CFTR currents.

First, I examined the role of intracellular calcium signaling utilizing the calcium chelater BAPTA and a pharmacological inhibitor of the IP_3R. I explored the role of STIM1 using STIM1-GFP to visualize translocation and shRNA to knock-down STIM1. I found that both free calcium and the IP_3R contributed to flagellin-induced CFTR currents, and that flagellin could cause STIM1 to translocate proximal to the plasma membrane. However, STIM1 shRNA failed to have any measurable effect on flagellin-induced CFTR currents. Lastly, I measured intracellular cAMP production using an ELISA and found that flagellin does not cause a measureable increase in whole cell cAMP levels.

In addition to calcium signaling, I also assayed the role of extracellular ATP in flagellin-induced CFTR currents. ATP is used as a paracrine signaling molecule in multiple systems and can induce the production of cAMP through GPCR receptors and activate a number of ion channels. Extracellular ATP and UTP both cause fluid and chloride secretion from cultured human airway epithelial cells (Benali *et al.*, 1994). Extracellular ATP has also been implicated in inflammatory signaling in asthma (Idzko *et al.*, 2007). Lastly, flagellin has been shown to cause ATP release by activating the signaling glycolipid asialoGM1 (McNamara *et al.*, 2001, Adamo *et al.*, 2004, McNamara *et al.*, 2006).

The ATP scavenging enzyme apyrase was utilized to remove free ATP from the extracellular bath. Suramin, an inhibitor of GPCR's and purinergic receptors, was utilized as well. Though apyrase appeared to have an effect in earlier pilot experiments, in a larger number of experiments apyrase did not have an effect on flagellin or forskolin induced currents. Suramin did strongly curtail flagellin-induced currents, but also prevented forskolin-induced currents, so the effect was likely non-specific. Overall, no evidence was found to support the notion that extracellular ATP was involved in flagellin-induced CFTR currents.

Lastly, I examined the role of PI3K signaling in flagellin-induced CFTR currents. It has been reported that flagellin causes activation of PI3K through TLR5 signaling as a mechanism

for reducing inflammatory signaling and hyperinflammation (Yu *et al.*, 2006). It has also been reported that inhibitors of PI3K reduce CFTR-mediated secretion in response to forskolin, which activates adenylate cyclase, and genistein, which binds and directly activates CFTR (Tuo *et al.*, 2009, Tuo *et al.*, 2011). The pharmacological inhibitor wortmannin was used to dampen PI3K activity and potassium bisperoxo(1,10-phenanthroline)oxovanadate (bpV) was used to inhibit Phosphatase and Tensin homolog (PTEN), the phosphatase that antagonizes PI3K activity. Wortmannin decreased the magnitude of flagellin-induced CFTR currents when applied after flagellin; bpV induced CFTR currents on its own, and flagellin increased the rate of current increase when used after bpV. Together this data indicated that the PI3K pathway may be involved in regulating flagellin-induced CFTR currents, however the effects may not be specific.

MATERIALS AND METHODS

Reagents

Unless otherwise stated, reagents were acquired from Sigma (St. Louis, MO). Purified, recombinant *P. aeruginosa* flagellin (Enzo Life Sciences, Farmingdale, New York) was reconstituted in water to 100µg/mL, aliquoted and stored at -80˚C. Individual aliquots were thawed and immediately used for each experiment. CFTR-172 inhibitor and forskolin were both prepared as 20mM stocks solutions in DMSO. Xestospongin C was reconstituted in ethyl alcohol at 1mM. Thapsigargin was prepared as a 5mM stock in DMSO. IBMX was prepared as a 100mM stock in DMSO. Apyrase powder was reconstituted in water to 2,000 Units/mL. Suramin was prepared as a 100mM stock in water. Wortmannin was prepared as a 1mM stock in DMSO. Potassium Bisperoxo(1,10-phenanthroline)oxovanadate (bpV) (EMD Millipore, Darmstadt, Germany) was prepared as a 10mM stock in water.

Cell Culture

Calu-3 cells were cultured in DMEM supplemented with 10% FBS, 1% pen-strep, and 2mM L-glutamine. For Ussing chamber experiments, cells were passaged onto 1.12-cm^2 permeable polycarbonate supports (0.4-µm pore size, Snapwell, Corning Costar, Cambridge, MA) and then grown until cells formed confluent monolayers. JME(CF15) nasal epithelial cells were cultured in DMEM/F-12 media supplemented with 10% FBS, 2 mM l-glutamine, 1% penicillin/streptomycin, 10 ng/mL EGF, 1 µm hydrocortisone, 5 µg/mL insulin, 5 µg/mL transferrin, 30 nM triiodothyronine, 180 µM adenine, and 5.5 µM epinephrine.

Transepithelial Electrophysiology

For measurements of transepithelial Cl^- current, Calu-3 cell monolayers were grown on permeable supports, washed in PBS, mounted into water-jacketed (37 °C) Ussing chambers (Physiologic Instruments, San Diego). Transepithelial voltage (V_t), resistance (R_t), and short circuit current (I_{SC}) were measured using typical four-electrode voltage clamp with Ag/AgCl electrodes (World Precision Instruments, Sarasota, FL) connected to the solutions through agar bridges containing 1M KCl. Positive currents were defined as cation movement from mucosa to serosa or anion movements in the opposite direction. Chamber compartments were separately perfused with 5 ml of Krebs-Henseleit solutions. A serosal-to-mucosal Cl^- gradient was used to increase the electrochemical driving force for Cl^- secretion across the apical membrane. The

basolateral solution contained (in mM) the following: 120 NaCl, 25 NaHCO$_3$, 5 KCl, 1.2 NaH$_2$PO$_4$, 5.6 glucose, 2.5 CaCl$_2$, and 1.2 MgCl$_2$. The mucosal Cl$^-$-free solution contained (in mM) the following: 120 sodium gluconate, 20 NaHCO$_3$, 5 KHCO$_3$, 1.2 NaH$_2$PO$_4$, 5.6 glucose, 2.5 Ca(gluconate)$_2$, and 1.2 MgSO$_4$. Solutions were gassed with 95% O$_2$ and 5% CO$_2$ resulting in pH 7.4. Voltage was clamped at 0mV across the epithelia with 1mV steps every 60 seconds to aid in observing transepithelial conductance. Transepithelial I$_{SC}$ measured under these conditions was termed I$_{Cl}$.

STIM1 TIRF Microscopy

JME cells were plated on cover glasses and incubated in growth media for 24 h before co-transfection with STIM1-GFP and CD8-tagRFP. Cells were allowed to express for 48 h before experiments were performed. Total internal reflection fluorescence measurements were made to exclude fluorescence from the ER, and CD8-tagRFP was utilized to focus exclusively on the cell's plasma membrane and ensure that the focal plane did not change during the course of the experiment. EGFP and tagRFP were alternately excited at 0.1 Hz by a 488-nm argon laser and 532-nm DPSS laser, respectively. Fluorescence emissions of GFP (525/50-nm bandpass filter, Chroma) and tagRFP (592/50-nm bandpass filter, Chroma) were acquired by an EMCCD camera (Andor iXon DV-897 BV) with 500-ms exposure per frame. Base-line images were acquired in standard Ringer's solution for 5 min before 1µg/mL flagellin was pipetted into the imaging chamber. 20 min after adding flagellin, 2µM thapsigargin was added, and images were taken for an additional 10 min. Fluorescence intensities were analyzed offline with ImageJ.

STIM1 RNAi

Plasmids expressing Stim1shRNA or non-silencing control shRNA from the GIPZ Lentiviral shRNAmir Library (Dr. Greg Hannon ,CSHL, and Dr. Steve Elledge, Harvard) were purchased from Thermo Scientific Open Biosystems (Huntsville, AL). Lentivirus particles were produced by transfecting HEK293T cells with the shRNA vectors along with the helper plasmid using the protocol from Nature Protocols 1, 241 - 245 (2006). The lentivirus was then used to infect Calu-3 cells and stable lines were established using puromycin selection.

cAMP ELISA

Competitive cAMP ELISA was performed using the cAMP-Screen® System (Applied Biosystems, Bedford, MA). Calu-3 cells were grown in 24 well plates and lysed with 100µL lysis buffer. Manufacturer protocol was followed utilizing 60µL per sample.

RESULTS

Intracellular calcium stores contribute to flagellin-stimulated currents, but STIM1 and cAMP production are not involved

Flagellin-induced chloride currents were measured by mounting Calu-3 human airway epithelia cells in an Ussing chamber (Fig. 1-1) (Li *et al.*, 2004a). Calu-3 cells were grown on permeable membranes until they formed an epithelial monolayer. The monolayers were then placed in an Ussing chamber, two-bath system with different solutions on the basolateral and

apical sides. A chloride gradient was established across the epithelial monolayer by using a high chloride solution in the basolateral bath and a chloride free solution in the apical bath. Electrodes in each bath were used to clamp voltage across the epithelium and measure chloride current through the use of a balancing short circuit current. Forskolin, an activator of ACs, was used in multiple experiments as a positive control for CFTR-mediated chloride currents, and CFTR-172 inhibitor was used to determine if CFTR was the current conductor. To examine the role of intracellular calcium signaling in flagellin-induced CFTR currents I began by employing an inhibitor of the IP_3R, Xestospongin C (XesC). Pretreatment of monolayers with 10μM XesC in the apical bath reduced the average magnitude of flagellin-induced CFTR currents by approximately 50% (Fig. 1-2 A,B). I then performed a similar experiment pre-treating Calu-3 cells for 90 minutes with the 20μM BAPTA-AM, a calcium chelator which enters the cell and becomes trapped. BAPTA pretreatment had a similar effect to XesC, reducing the magnitude of flagellin-induced chloride currents (Fig1-2 C,D). Adding flagellin and XesC or BAPTA at the same time also altered the normal dynamics of the response. Monolayers that responded strongly to flagellin exhibited oscillations in current magnitude with peaks occurring between 10 and 20 minutes apart (Fig. 1-1,1-2). XesC or BAPTA-treated cells exhibited either smaller oscillations or no oscillations with a plateau once maximum current was reached, perhaps indicating that the oscillations in chloride current were the result of oscillations in cytosolic calcium. Though there are many examples of calcium oscillations in the literature (Dupont *et al.*, 2011), calcium oscillations with a period of more than 10 minutes would be novel.
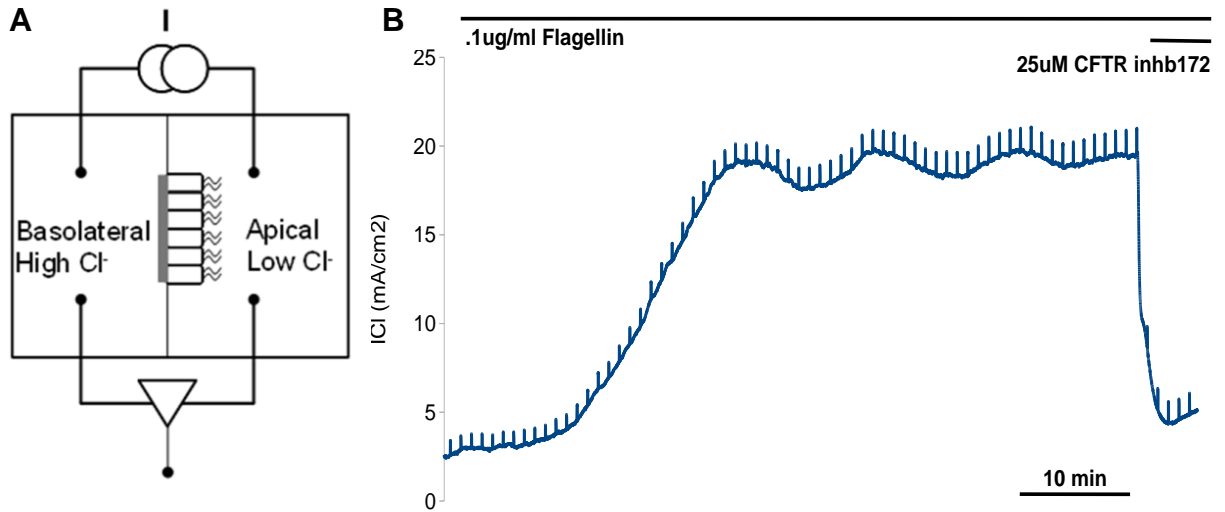
Figure 1-1. Flagellin induces chloride current through the CFTR. (**A**) Setup for Calu-3 monolayers in Ussing chambers with high basolateral chloride and low apical chloride, voltage clamp and short-circuit current. Image courtesy of C. Schwarzer. (**B**) Calu-3 monolayers exposed to apical .1μg/mL flagellin followed by 25uM CFTRinhb172. Current trace is representative of numerous experiments.
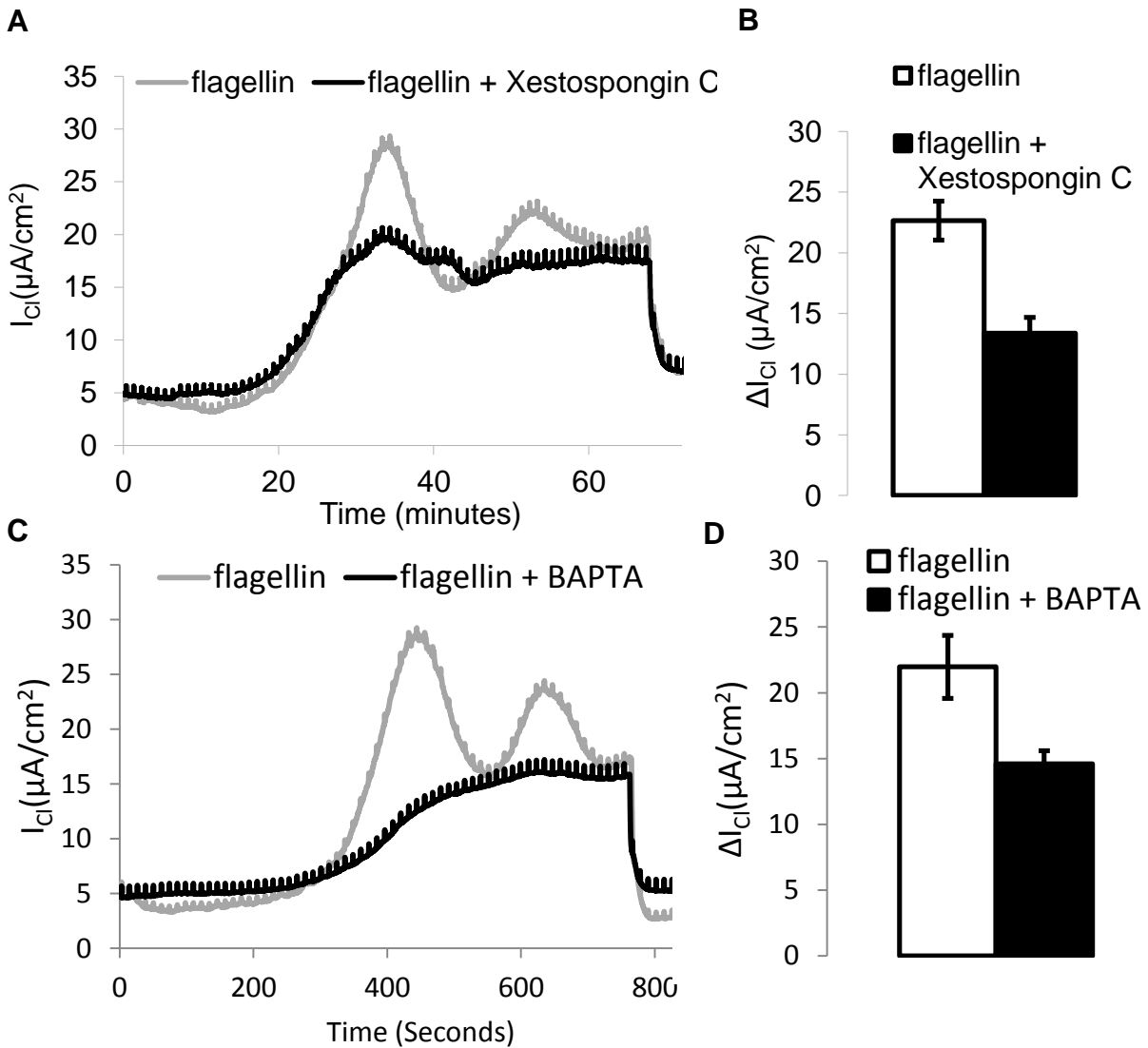
Figure 1-2. Xestospongin C and BAPTA reduce the amplitude of flagellin-induced CFTR currents. (**A**) Calu-3 monolayers mounted in Ussing chambers with high basolateral chloride and low apical chloride exposed to apical .1µg/mL flagellin or flagellin with 10uM Xestospongin C followed by 20µM CFTR172 inhibitor. Representative current traces. (**B**) Maximum change in current displayed as group averages from (A) with error bars representing standard error. N=3 biological replicates for each treatment. (**C**) Calu-3 monolayers either pretreated for 90 min with 20µM BAPTA-AM or untreated and mounted in Ussing chambers and exposed to apical .1µg/mL flagellin followed by 20µM CFTR172 inhibitor. Representative current traces. (**D**) Maximum change in current displayed as group averages from (C) with error bars representing standard error. N=3 biological replicates for each treatment.

Given the implicated role of the IP$_3$R, I next examined the role of the ER calcium sensor STIM1. JME nasal epithelial cells were transfected with STIM1-GFP and imaged using TIRF fluorescence. In this system, an increase in fluorescence signal implies that STIM1 is translocating proximal to the plasma membrane, a necessary step in its activated signaling pathway. In most experiments, 1µg/mL flagellin caused an increase in STIM1-GFP TIRF signal (Fig. 1-3). The addition of the SERCA blocker thapsigargin, which lowers ER calcium levels by inhibiting the pump used to refill the ER, caused an increase in STIM1-GFP TIRF signal that was roughly 2-3 times that of flagellin. These data indicated that flagellin was releasing a fraction of stored calcium from the ER and partially activating STIM1, a requirement for activating SOCE and/or SOcAMP. Thapsigargin fully releases ER calcium and further increases STIM1 activation. This experiment however comes with a number of caveats. In this experiment, STIM1 was overexpressed, perhaps leading to enhanced sensitivity to minor changes in ER calcium levels. Since STIM1 is held inactive by free Ca^{2+} in the ER lumen, more STIM1 would require more Ca^{2+} to prevent activation and could lead to higher baseline STIM1 activation and increased sensitivity to small changes in Ca^{2+}. Flagellin also failed to induce a response in several experiments, including many in which thapsigargin continued to have an effect.

As a further test of the role of STIM1 in flagellin signaling, I utilized Calu-3 cells prepared by Zhu Fu which had been infected with STIM1 shRNA via a lentiviral vector. The efficacy of the shRNA was measured by RT-PCR and through a functional assay. The functional assay consisted of placing STIM1 shRNA and scrambled shRNA Calu-3 monolayers in Ussing chambers, inducing a maximal CFTR current using forskolin, and then measuring responses to thapsigargin which induces a current through calcium-gated chloride channels. In scrambled shRNA Calu-3 monolayers, thapsigargin induced sequential increases in chloride current (Fig. 1-4). The first increase likely resulted from release of calcium into the cytosol from the ER, activating Ca^{2+}-activated chloride channels (CaCC) in the apical plasma membrane to directly increase chloride current and/or Ca^{2+}-activated potassium channels in the basolateral membrane that hyperpolarize the cell and drive chloride across the apical membrane through either CFTR or CaCC. The second phase of the current response to thapsigargin likely resulted from STIM1 activating ORAI and allowing calcium to enter the cytosol from the extracellular bath. In STIM1 shRNA Calu-3 cells the first current increase from thapsigargin was present and similar to scrambled shRNA. However, the second increase in current attributed to STIM1 was absent or greatly muted in all STIM1 shRNA Calu-3 monolayers, indicating a functional knockdown of STIM1. With this information, I went on to treat STIM1 shRNA and scrambled shRNA Calu-3 monolayers with 0.1µg/mL flagellin (Fig. 1-5). There was no difference in flagellin-induced CFTR currents between STIM1 and scrambled shRNA Calu-3 cells, indicating that functional STIM1 was likely not required for flagellin-induced CFTR currents.
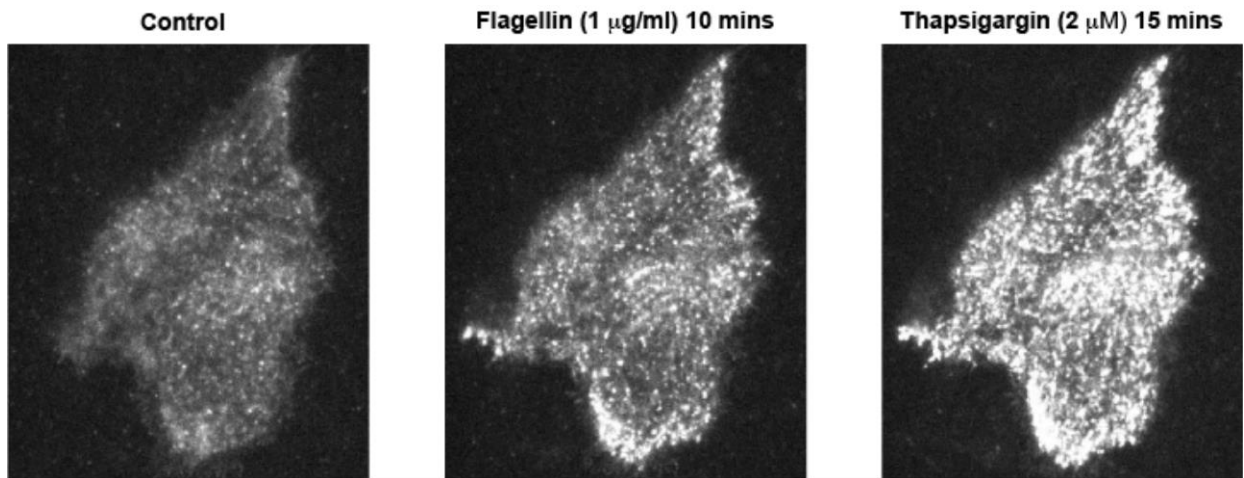
Figure 1-3. Flagellin recruits STIM1 to membrane. JME cells transfected with STIM1-GFP and imaged using TIRF microscopy with indicated treatments. Representative of multiple experiments. Data courtesy of Ryan Arant (UC Berkeley).
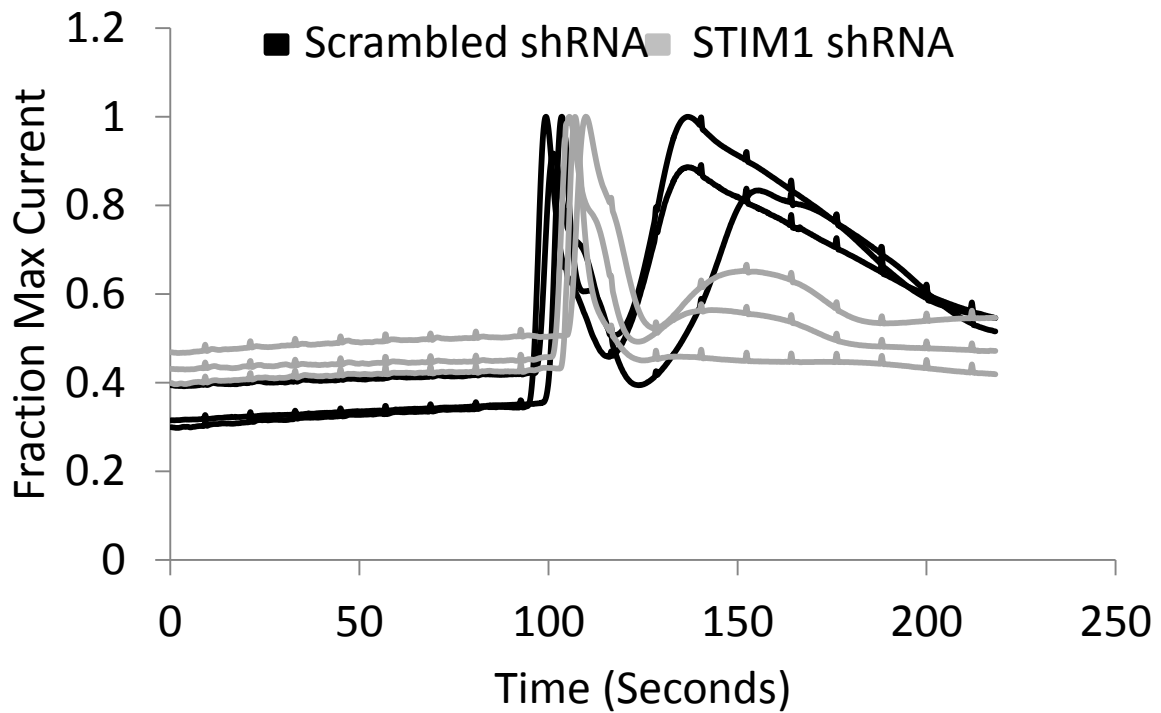
Figure 1-4. STIM1 shRNA functionally knocks down STIM1. Calu-3 cells transformed with STIM1 or scrambled shRNA mounted in Ussing Chambers and treated with 20uM Forskolin (before data collection) and 5uM Thapsigargin at 100 seconds. Displayed as fraction maximum current for better peak alignment. Average starting currents for scrambled shRNA 74.59 $\mu A/cm^2$ and STIM1 shRNA 81.08 $\mu A/cm^2$.
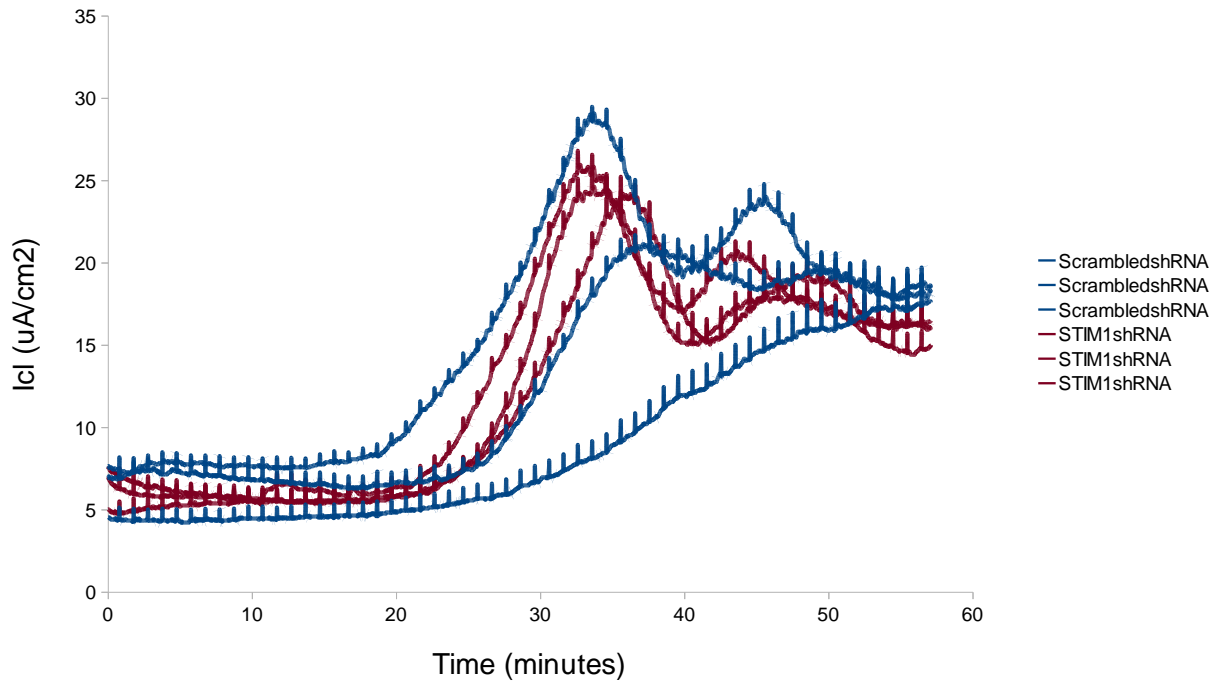
Figure 1-5. STIM1 shRNA does not prevent flagellin-induced CFTR currents. Calu-3 monolayers transformed with either STIM1 shRNA or scrambled shRNA mounted in Ussing Chamber with high basolateral chloride and low apical chloride exposed to apical .1µg/mL flagellin. Current traces from three biological replicates per cohort displayed, representative of 6 total replicates per cohort.

To test the final part of the SOcAMP hypothesis, that flagellin was eventually causing cAMP production, I performed a cAMP ELISA. The idea that flagellin was inducing cAMP production was based on experiments showing that the addition of a competitive inhibitor to cAMP, RpBrcAMPS, prevented CFTR responses to flagellin. However, ELISA experiments in Calu-3 cells showed no increase in cAMP levels in flagellin treated cells, even in the presence of the PDE inhibitor IBMX (Fig. 1-6). Calu-3 cells treated with forskolin in the same experiment showed a 50-fold increase in cAMP levels.

There are three possible explanations for the difference between the RpBrcAMPS data and the ELISA data. The first is that the ELISA assay is insufficiently sensitive to measure small, local changes in cAMP that may activate PKA adjacent to nearby CFTR at the apical membrane (Sun *et al.*, 2000, Naren *et al.*, 2003).

A second possible explanation for the apparent discrepancy between the ELISA data and the electrophysiological data with RpBrcAMPS is centered around the fact that the current response to flagellin in Calu-3 cells is inconsistent. Current measurements in response to flagellin often yielded minimal or no responses. As much of the variance in flagellin response occurred from one day to the next, the inconsistency could be accounted for in electrophysiological experiments by using multiple replicates and only taking data from days in which control experiments consistently showed a strong response to flagellin. In the ELISA experiment we have no way of knowing whether or not CFTR currents were elicited in these cells, so the lack of cAMP production may just be because no flagellin response occurred.

A third possibility is that RpBrcAMPs reduces PKA activity that is required for flagellin to trigger an increase in current, i.e., cAMP is necessary but not sufficient for flagellin-activation of CFTR. This possibility is consistent with the data in the literature that shows that CFTR excised in patches and removed from PKA loses conductance in seconds (Becq *et al.*, 1994). Thus, even if flagellin were not acting through cAMP/PKA, a drop in PKA activity might greatly hinder CFTR currents of all types.

Overall, these data were inconclusive about the role of PKA in regulating CFTR in response to flagellin stimulation. The possibility still exists that PKA, PKC or cGKII may be effectors in this response.
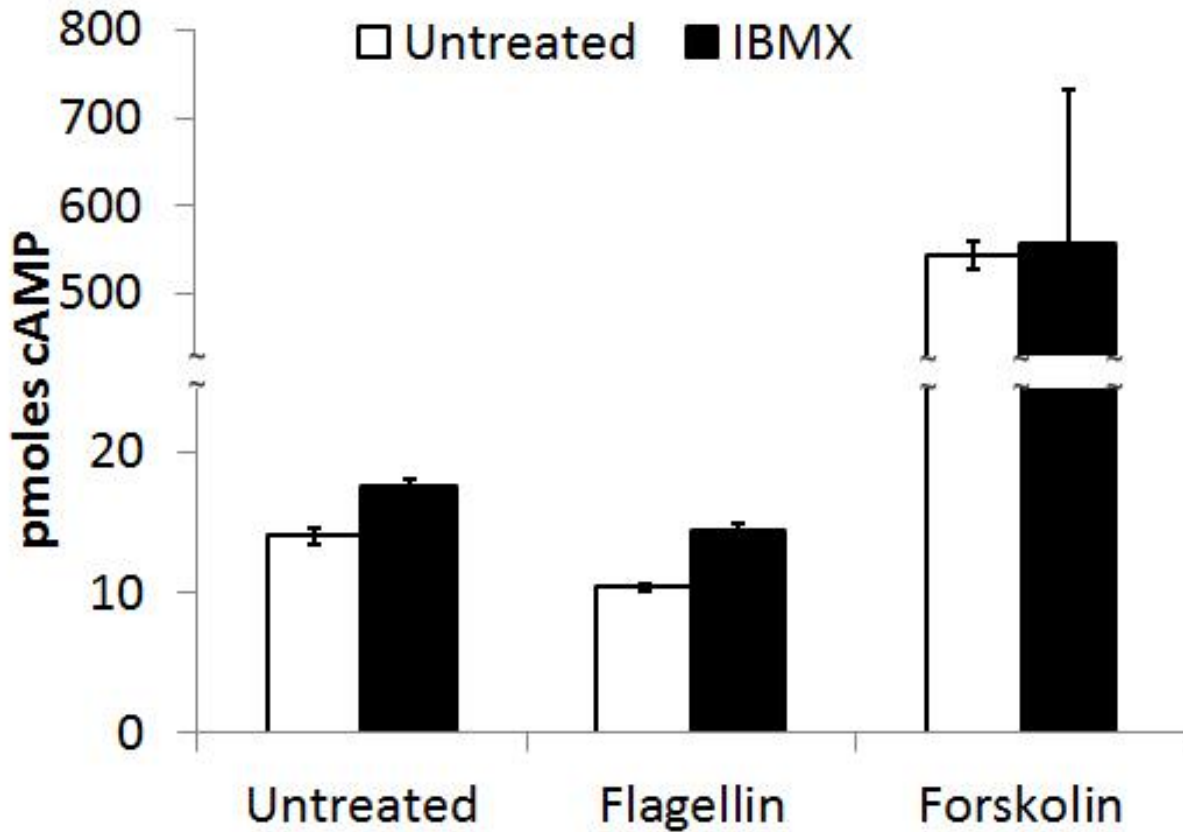
Figure 1-6. Flagellin does not cause measureable cAMP increases in bulk extracts. Calu-3 cells pretreated for 30 minutes with 50μM IBMX (PDE Inhibitor) followed by 30 minutes with 1μg/mL Flagellin or 20μM Forskolin added. Cell extracts were taken and cAMP ELISA was performed with standards. N=3 biological replicates, error bars indicate standard error.

Extracellular ATP is not required for flagellin-induced CFTR currents

Next, I examined the role of paracrine ATP signaling in flagellin responses. The ATP scavenging enzyme apyrase was added to the apical bath before flagellin treatment. Although an initial experiment from Bharat Ravishankar showed a repression of the flagellin response under these conditions, this conclusion was based on only one replicate. When I repeated the experiment, I saw no correlation between the presence of apyrase and the magnitude of flagellin or forskolin responses (Fig 1-7). In addition to the experiments with apyrase, suramin, an inhibitor of purinergic receptors and GPCRs, was also tested for its efficacy in preventing flagellin-induced CFTR currents. Though suramin added to the basolateral bath did prevent flagellin-induced CFTR currents, it also greatly reduced the size of forskolin responses, so the inhibitory effect may not have been specific to flagellin signaling (Fig 1-8). The fact that suramin was only effective when added to the basolateral bath suggests that it must be acting on a protein in the basolateral membrane. I could find no explanation for this effect based on published interactions of suramin. One novel possibility is that it is in an inhibitor of the Na-K-Cl cotransporter (NKCC), which is in the basolateral membrane and is required for chloride transport across the epithelium. Taken together, the lack of a phenotype observed with apyrase treatment and the non-specific effect seen from suramin indicated that paracrine ATP signaling may not have been involved in flagellin-induced CFTR currents.
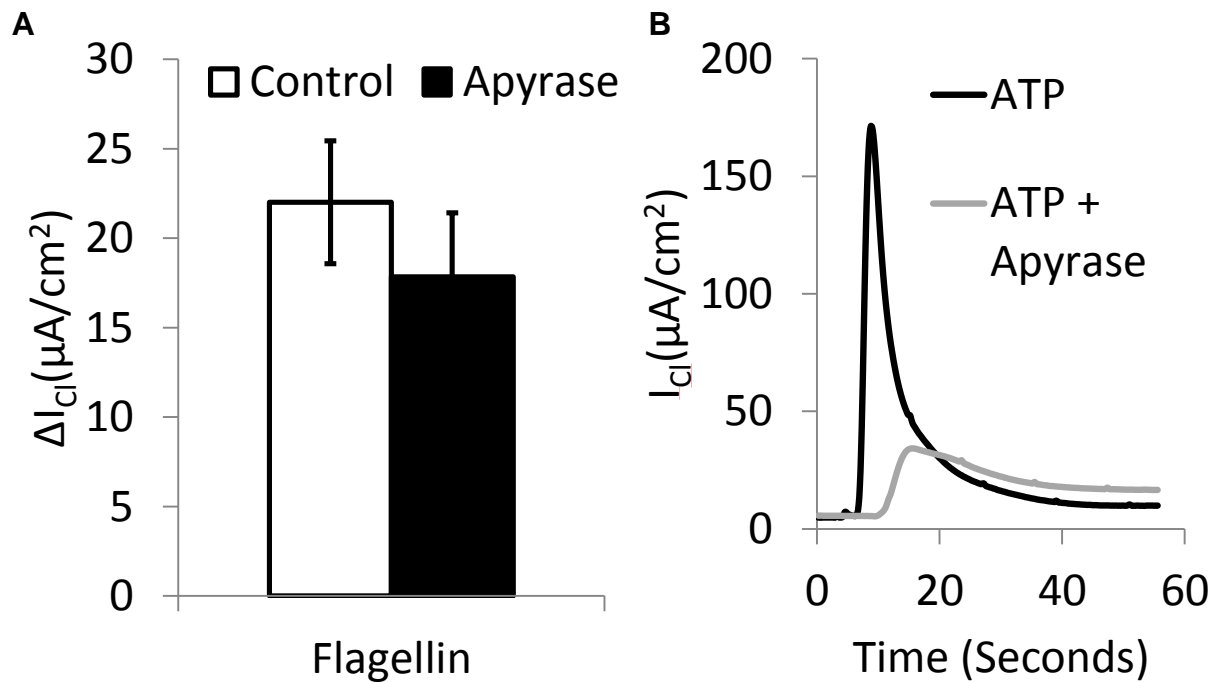
Figure 1-7. Apical apyrase has no effect on flagellin-induced chloride currents. (**A**)Calu-3 cells mounted in Ussing Chambers and treated apically with buffer control or 2 U/mL apyrase followed by .1 µg/mL flagellin and then 20µM forskolin. Data displayed as average changed in current from pre-treatment minimum to post-treatment maximum. N=3 biologicals replicates, error bars indicate standard error. (**B**) Calu-3 cells mounted in Ussing chambers with 50µM ATP or 50µM ATP preincubated for 10min with 2 U/mL apyrase applied to basolateral bath.
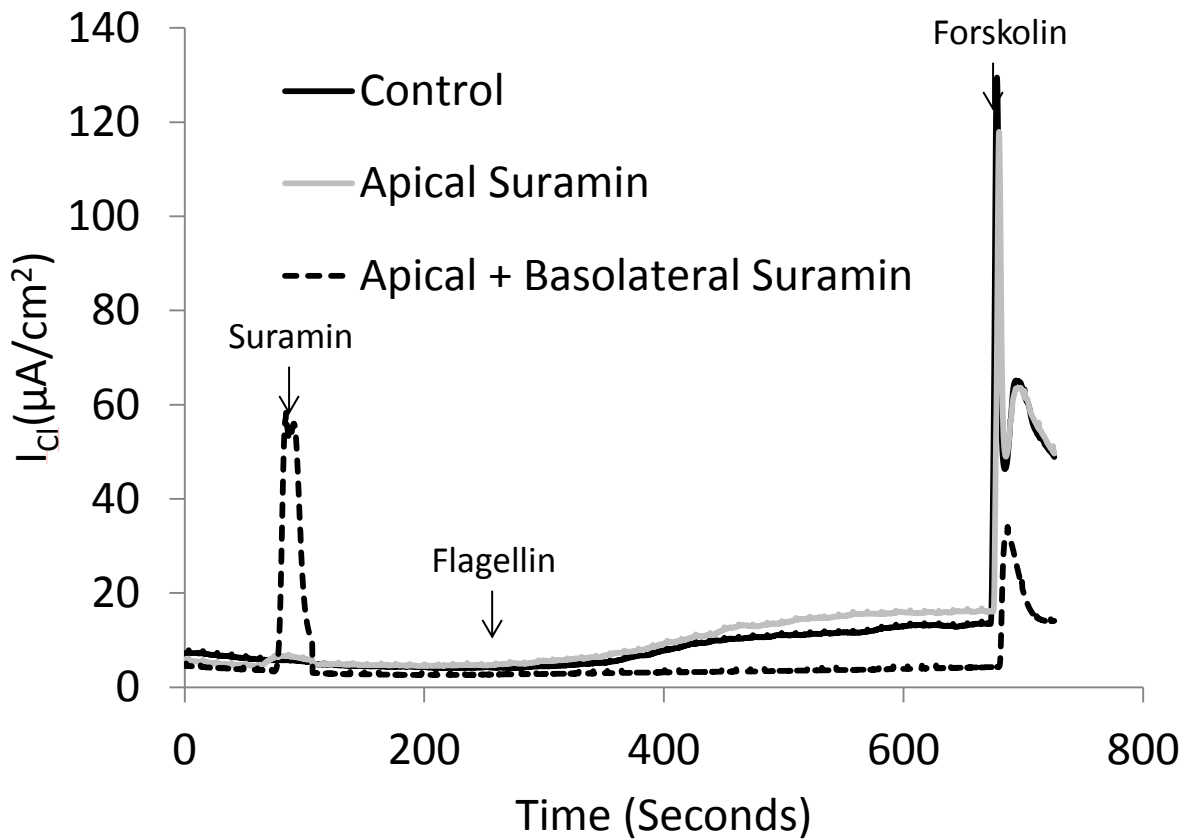
Figure 1-8. Basolateral Suramin has a non-specific effect on chloride currents. Calu-3 cells mounted in Ussing Chambers and either untreated, treated with 1mM apical suramin or .5mM apical and basolateral Suramin followed by .1 µg/mL flagellin and then 20µM forskolin. Representative traces from three experiments plotted.

Flagellin and the PI3K pathway

Lastly, I examined interaction between flagellin-induced chloride currents and the PI3K pathway. When applied to the apical bath after flagellin stimulation, wortmannin, the PI3K inhibitor, caused a decrease in chloride current (Fig. 1-9). However, wortmannin treatment also caused a more than 50% reduction in forskolin induced chloride currents. This finding is consistent with previous published work (Tuo *et al.*, 2009, Tuo *et al.*, 2011). This result suggests that wortmannin's effect on flagellin currents may not be specific. I further explored the role of the PI3K pathway with the PTEN inhibitor bpV. PTEN is the phosphatase which antagonizes PI3K, so inhibiting PTEN should have a similar effect to activating PI3K. bpV caused an increase in chloride currents in Calu-3 cells which was partially inhibited by CFTR-172 inhibitor, however chloride currents continued to increase after the addition of the inhibitor with increasing conductance as seen during the voltage steps (Fig. 1-10). Addition of flagellin after bpV increased the rate with which both the chloride current and conductance increased. The large conductance observed was consistent with the breakdown of epithelial integrity, either through cell death or the loss of tight junction integrity. The caspase inhibitor ZVAD was utilized to examine the role of programmed cell death. Pretreatment with ZVAD failed to prevent the large conductance caused by bpV and flagellin, suggesting that this effect was likely due to the loss of tight junction integrity, not due to caspase-dependent programmed cell death. This is consistent with published work which has shown that PI3K co-immunoprecipitates with occludin and PI3K inhibition increases epithelial and endothelial barrier function during conditions of inflammatory stimulation or oxidative stress (Sheth *et al.*, 2003, Cain *et al.*, 2010). Taken together, these data reflect that flagellin likely causes activation of PI3K and that this activity may be involved both in CFTR-dependent chloride conductance and loss of tight junction barrier function.
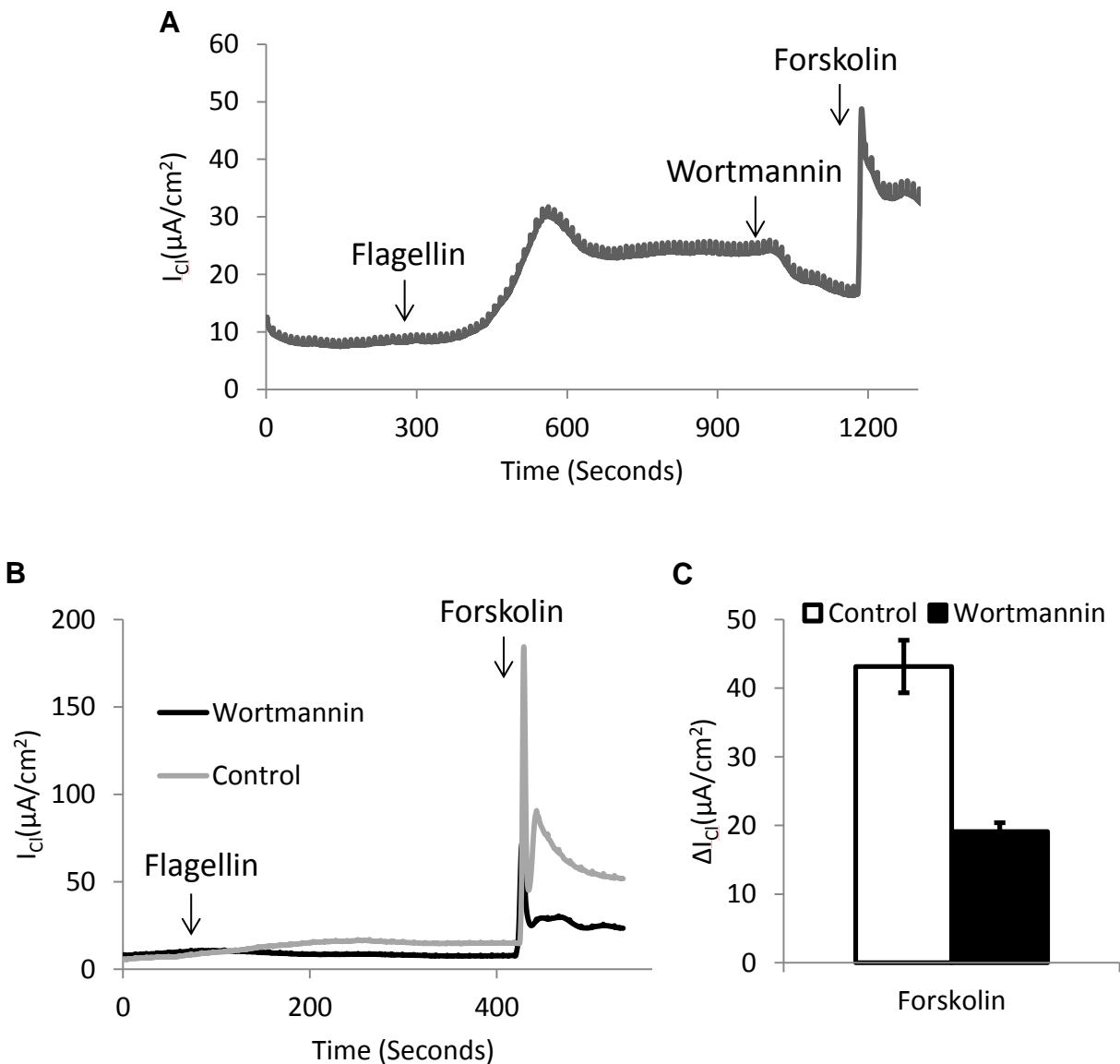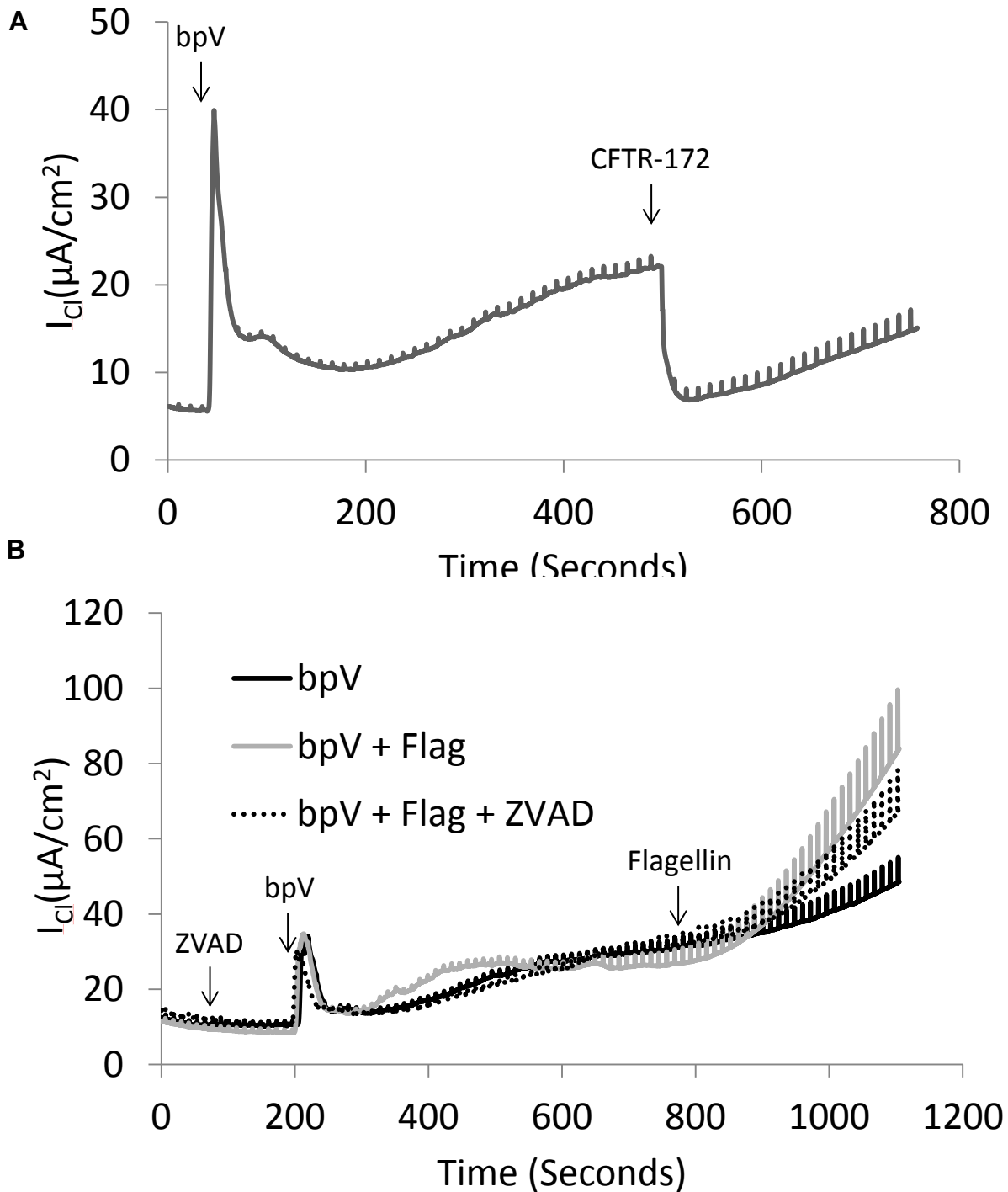
Figure 1-9. Wortmannin inhibits Flagellin-induced and Forskolin-induced chloride currents. (**A**) Calu-3 cells mounted in Ussing Chambers and treated apically with .1 µg/mL flagellin followed by 100nM Wortmannin and then 20µM Forskolin. Representative trace from three experiments plotted. (**B**) Calu-3 cells mounted in Ussing Chambers and either untreated or treated apically with 100nM Wortmannin followed by .1µg/mL Flagellin and 20µM Forskolin to both groups. Representative traces. (**C**) Average change in current (after plateau) from (B) plotted for Forskolin addition. N=3 biological replicates, error bars indicate standard error.

Figure 1-10. bpV induces CFTR-dependent and CFTR-independent chloride currents.
(**A**) Calu-3 cells mounted in Ussing Chambers and treated apically with 100μM bpV followed
by 20μM CFTR-172 inhibitor. Representative trace from three experiments plotted. (**B**)
Calu-3 cells mounted in Ussing Chambers and treated with apical and basolateral 50μM
ZVAD, apical 50μM bpV and apical .1 μg/mL Flagellin. Representative traces from three
experiments per condition plotted.

DISCUSSION

In this study I have explored possible mechanisms for flagellin-induced chloride currents in human airway cells. I found that intracellular calcium signaling may have contributed to, but was not necessary for, flagellin-induced chloride currents. This was evidenced by the smaller magnitude currents observed when cells were treated with XesC, an inhibitor of the IP_3R, or the calcium chelator BAPTA. I found that STIM1 may be recruited to the plasma membrane during flagellin exposure, however STIM1 shRNA experiments failed to have any effect on flagellin-induced chloride currents. I also failed to find any new evidence of cAMP production in response to flagellin as measured through an ELISA, though this does not preclude smaller, local changes regulating PKA and CFTR activity. Apyrase, the ATP scavenging enzyme, had no effect on flagellin responses, and suramin, a purinergic receptor angtagonist, had only non-specific effects on chloride currents, leading to the conclusion that paracrine ATP signaling was not necessary for flagellin-induced chloride currents. Lastly, through the use of kinase and phosphatase inhibitors, I found that PI3K activity may contribute to flagellin-induced chloride currents, though this effect may be due to regulation of tight junction barrier integrity, not the CFTR.

The connection between known flagellin signaling pathways and CFTR regulation remains unclear. There is no established signaling pathway that links TLR5 activation to adenylate cyclase activity. Adenylate cyclases are most commonly activated by G-protein coupled receptors (GCPRs), suggesting that TLR5-induced autocrine signaling of some form may lead to adenylate cyclase activation (Hanoune *et al.*, 2001). This study suggests that if autocrine signaling is responsible flagellin-induced chloride currents, the signaling molecule is unlikely to be ATP. Adenylate cyclases can also be activated in multiple ways through intracellular calcium signaling. In addition to free calcium and calmodulin, it has been reported that drops in ER calcium can lead to adenylate cyclase activity through activation by the ER calcium sensor STIM1 (Lefkimmiatis *et al.*, 2009). This study offers evidence that cytosolic calcium released from the ER through the IP_3R may contribute to flagellin-induced chloride currents, however STIM1 does not appear to be necessary for this effect. This suggests that signaling from TLR5 may lead to ER calcium release, and this has been observed in response to flagellin in the literature (McNamara *et al.*, 2006), however the known pathway leading from TLR5 to ER calcium involves autocrine ATP signaling, which I found no evidence for in this study. I did find evidence that PI3K activity contributes to flagellin-induced chloride currents, and PI3K is known to be activated by TLR5 signaling to reduce inflammatory gene expression (Yu *et al.*, 2006), however PI3K inhibitors also reduce chloride secretion induced by forskolin. The loss of epithelial integrity observed with bpV treatment indicates that the effects of PI3K on flagellin-induced chloride currents may be the result of altered tight junction barrier function.

From this study I conclude that cytosolic calcium and PI3K activity contribute to flagellin-induced chloride currents, though neither appears to be necessary, and PI3K activity may not relate to CFTR-dependent currents. This remains an interesting field a study with the possibility of discovering a novel pathway linking flagellin receptors to CFTR activity, however this research is severely hindered by the inconsistent response to flagellin I observed in Calu-3 cells. Attempts to study flagellin-induced chloride currents in CFTR-corrected CFBE cells were even less promising. Until a reliable system for studying this effect can be discovered, it will

remain a very difficult task to decipher the signaling cascade which leads from flagellin exposure to CFTR-dependent chloride secretion.

Chapter 2

Effects on immune signaling of *Pseudomonas aeruginosa* quorum sensor HSL-C12

INTRODUCTION

Pseudomonas aeruginosa are gram-negative bacteria that form biofilms in the airways of patients with Cystic Fibrosis (CF) (Hoiby *et al.*, 1977). *P. aeruginosa* coordinate the production of biofilms using the small molecule N-(3-oxododecanoyl)-homoserine lactone (HSL-C12) as a diffusible quorum-sensing molecule (Schuster *et al.*, 2006, Rumbaugh, 2007, Irie *et al.*, 2008). HSL-C12 has multiple effects on mammalian cells, including inducing apoptosis and activating store-operated calcium signaling (Tateda *et al.*, 2003, Li *et al.*, 2004b, Jacobi *et al.*, 2009, Li *et al.*, 2009, Schwarzer *et al.*, 2010, Schwarzer *et al.*, 2012). HSL-C12 has also been reported to affect inflammatory signaling, though some reports indicate an activation of pro-inflammatory signaling while others indicate a suppression of inflammatory signaling (Telford *et al.*, 1998, Smith *et al.*, 2001, Smith *et al.*, 2002, Kravchenko *et al.*, 2006, Jahoor *et al.*, 2008, Kravchenko *et al.*, 2008).

The goal of this study was to elucidate HSL-C12's role in inflammatory signaling and discover associated effector molecules. To accomplish this we used mouse embryonic fibroblasts (MEF). Fibroblasts are expected to be exposed to the membrane-permeant HSL-C12 in *P. aeruginosa* biofilm-infected lungs. In addition, MEF are a genetically tractable system with many knockout lines available. We measured expression and secretion of KC, the mouse equivalent of human IL-8, because it is an important cytokine mediating epithelial immunity produced in response to NF-κB signaling. TNFα and IL-1β were utilized as potent activators of the NF-κB pathway. We found that HSL-C12 increased KC gene expression, but prevented KC secretion, even in the presence of TNFα or IL-1β. This uncoupling of gene expression from secretion appeared to result from an inhibition of protein synthesis. Because HSL-C12 is known to release Ca^{2+} from the endoplasmic reticulum (ER) (Shiner *et al.*, 2006, Schwarzer *et al.*, 2010, Schwarzer *et al.*, 2012) and reductions in ER $[Ca^{2+}]$ trigger ER stress (Kaufman, 1999), we explored the role of ER stress transducers in HSL-C12-mediated translation inhibition.

PERK, a kinase embedded in the ER membrane, is one of four kinases known to phosphorylate the eukaryotic translation elongation factor eI-F2α (Harding *et al.*, 1999). PERK becomes activated when BiP chaperone proteins, which usually inhibit PERK, release PERK and are sequestered to the ER lumen due to a buildup of unfolded proteins (Bertolotti *et al.*, 2000). eI-F2α is a translation elongation factor which, when phosphorylated on serine 52 (51 in human), causes selective inhibition of protein synthesis and allows only certain chaperones and ER stress response proteins to be translated (Hinnebusch, 1994). We observed that HSL-C12's stimulation of KC gene expression and inhibition of KC secretion in WT and PERK-corrected PERK^{-/-} MEF were greatly reduced in PERK^{-/-} MEF. HSL-C12 also caused an increase in KC secretion in a PERK-dependent manner in longer treatment regimens. Together these data suggest that HSL-C12, through its effector PERK, reduces KC secretion in the short term but could contribute to a hyper-inflammatory state in the long term.

MATERIALS AND METHODS

Reagents

Unless otherwise specified, reagents and chemicals were obtained from Sigma. HSL-C12 (Cayman Chemical, Ann Arbor MI and Sigma) was dissolved in DMSO as 50mM stock ad freeze thaw cycles were limited. HSL-C12 from different suppliers displayed different activities and therefore 50uM or 100uM doses were used accordingly. TNFα and IL-1β (both R&D Systems, Minneapolis, MN) were used at 10ng/mL from 10μg/mL stock solutions in water. The Ca^{2+}-ATPase blocker thapsigargin (Christensen *et al.*, 1993) was prepared as a 1 mM stock in DMSO and used at 1 μM.

Cell Culture of MEF

WT MEF were obtained from C. Li (Univ. Louisville). PERK^{-/-} and corresponding PERK-corrected PERK^{-/-} MEF cells lines were obtained from R. Kaufman (Sanford|Burnham Medical Research Institute). MEF were cultured in Dulbecco's Modified Eagles Medium (DMEM) containing 10% FBS and 1% penicillin-streptomycin. The cells were passaged at 1:5-1:15 dilutions and the remaining cell suspension was seeded directly onto a 24-well, 12-well or 6-well tissue culture plate (BD Falcon, Bedford, MA).

ELISA and quantitative PCR for KC

WT, PERK^{-/-} and PERK-corrected PERK^{-/-} MEF were grown to confluency on 24-well plates, and experimental cells were treated for 4hrs with HSL-C12 (50 μM), TNFα (10-20 ng/ml), IL-1β (10ng/mL) or HSL-C12 in combination with TNFα or IL-1β. The cell culture medium was removed, the cells were washed with PBS, and samples were taken using TRIzol reagent (Life Technologies, Grand Island, NY). ELISAs were performed using R&D Systems Duo Set® kit (R&D Systems, Minneapolis, MN). Capture antibodies were incubated on Nunc MaxiSorp 96-well plates in 0.1M sodium phosphate buffer pH 8.0 overnight at 4°C, and then the plates were blocked with DPBS with 1% BSA (PBSA) for 4hrs at 4°C. 50uL of culture media per well were taken from the MEF's and applied to the plate overnight at 4°C, followed by five washes with PBS with 0.1% Tween-20 (PBST) and biotinylated capture antibodies in PBSA for 2 hrs at room temperature. Five more PBST washes were performed followed by 30 mins of streptavidin-HRP at room temperature. After five more PBST washes wells were developed for 10 min at room temperature in the dark with 1mg/ml OPD in 0.05M sodium phosphate/0.02M Citrate buffer, pH 5.0 and stopped with 3M HCl. Absorbance was read in a spectrophotometer at 490nm.

Extensive cell death in longer HSL-C12 treatments required that the KC ELISA be normalized to cell number. This was accomplished by normalizing to [protein] adherent to the cell culture plate after washing. Samples were taken from organic phase from TRIzol preparation and dot-blotted onto filter paper. Filter paper was then stained with Coomassie Blue and then destained with 10% methanol 10% acetic acid. Filter paper was then scanned and quantified using ImageJ. KC concentrations obtained through ELISA were then divided by [protein] acquired through dot-blot. This normalization was only performed for experiment in Figure 7.

For qPCR experiments, purified RNA samples from TRIzol lysates were treated with DNase (Frementas, Glen Burnie, Maryland) and then reverse transcribed using SuperScript III

(Life Technologies, Grand Island, NY) with random primers. KC gene expression level was determined by real-time PCR carried out in 7900HT Fast Real-Time PCR System (Applied Biosystems) with SYBR mix (KAPA Biosystems, Woburn, MA) using gene-specific primers. House-keeping gene Rps17 was used as normalization control throughout all experiments, and all data are presented as RQ score relative to RPS17. Primers used for real-time PCR were: KC: forward: 5′-CTTGAAGGTGTTGCCCTCAG-3′ and reverse: 5′-TGGGGACACCTTTTAGCATC-3′. Rps17: forward: 5'-CGCCATTATCCCCAGCAAG-3' and reverse: 5'-TGTCGGGATCCACCTCAATG-3'

Western Blotting

MEF were grown in 6-well plates to confluency and treated for up to 4 hours with HSL-C12 or 1 hour with 1µM thapsigargin and then lysed in M-PER mammalian protein extraction reagent (Pierce, Rockford, IL) containing 5 µg/ml leupeptin, 5 µg/ml pepstatin, 1 mM phenylmethylsulfonyl fluoride, and 50 nM calyculin A. Protein sample concentrations were determined with Bradford reagent (Bio-Rad, Hercules, CA). Immunoblot analysis was performed by first separating protein (10 to 50 µg/lane) by sodium dodecyl sulfate-polyacrylamide gel electrophoresis and subsequently transferring it to nitrocellulose membranes. Individual gels with identical loading were run side by side when multiple primary antibodies were utilized. Membranes were blocked (5% nonfat dried milk) in 20 mM Tris-HCl (pH 7.5)-150 mM NaCl-0.1% Tween 20 for 1 hour and then incubated with specific antibodies overnight. Primary antibodies (diluted 1:1,000 in blocking buffer) for phosphoS51- eI-F2α (119A11), eI-F2α (9722), IκBα (L35A5), and NF-κB p65 (C22B4) were acquired from Cell Signaling (Danvers, MA). Binding of primary antibodies was visualized by enhanced chemiluminescence with horseradish peroxidase-conjugated secondary antibodies (1:2,500 in blocking buffer) and Renaissance Chemiluminescence Reagent Plus (Perkin-Elmer Life Sciences). Quantitation was performed with ImageJ (National Institutes of Health, Bethesda, MD).

^{35}S *uptake into protein*

Figure 2-2: WT MEF were grown in 24-well plates to confluency. Wells were pretreated for 3hrs with either 50µM HSL-C12 or DMSO (control). At 3hrs post-infection, medium was removed and incubated with 25 µCi/ml [^{35}S]methionine (Perkin Elmer, Waltham, MA) in RPMI 1640 medium without methionine supplemented with 10% serum, 2 mM L-glutamine, and 50µM HSL-C12 or DMSO. Cells were labeled for 1hr, washed three times with cold PBS, and then lysed with radioimmunoprecipitation assay (RIPA) buffer supplemented with 2 mM Na$_3$VO$_4$, 1 mM PMSF, 25 mM NaF, and 1x Roche protease inhibitor mixture (no EDTA) (pH 7.2) for 10 min at 4°C. Total protein levels were measured by bicinchoninic acid assay, and equal amounts of protein were mixed with SDS sample buffer (40% glycerol, 8% SDS, 2% 2-ME, 40 mM EDTA, 0.05% bromophenol blue, and 250 mM Tris-HCl [pH 6.8]), boiled for 5 min, and then separated by SDS-PAGE. The gels were stained with Coomassie blue to show equal protein loading, dried, and exposed to a phosphor screen and visualized using a Typhoon Trio imager (GE Healthcare).

Figure 2-5: Same as Figure 2, with treatments of 100uM HSL-C12 combined with 10ng/mL TNFα for 3 or 7 hours pre-labeling. Phosphor and coomassie images were quantified using ImageJ (NIH, Bethesda, MD).

RESULTS

Short Exposures to HSL-C12 Reduces KC Secretion and Inhibits Protein Synthesis

In order to determine HSL-C12's effects on inflammatory signaling in MEF we measured both cytokine gene expression using quantitative PCR (qPCR) and protein secretion into the cell medium using ELISA. MEF were treated for 4 hours with HSL-C12 (50µM), TNFα (10ng/mL) or a combination of the two. Results have been summarized in Figure 2-1. TNFα caused an increase in both KC gene expression and secretion as expected. In contrast, HSL-C12 caused increases in KC gene expression but decreased KC secretion. When TNFα was given in combination with HSL-C12, KC gene expression increased but KC secretion decreased when compared to TNFα alone. Similar results were obtained when IL-6 secretion and gene expression were measured by ELISA and qPCR, respectively (data not shown).

The decoupling of gene expression and protein secretion caused by HSL-C12 could have been due to either a block of KC protein synthesis or an inhibition of protein secretion. To distinguish between these two possibilities we utilized a ^{35}S-methionine metabolic labeling approach to measure global translation levels in MEF after treatment with HSL-C12 (Fig. 2-2). During the final hour of HSL-C12 or DMSO 4 hour treatments on WT MEF's, the media were replaced with media in which the only source of methionine was radioactive ^{35}S-methionine. Any new proteins synthesized during this time would incorporate radioactive methionine, and the level of incorporation will be directly proportional to the amount of translation occurring in those cells. When protein samples were taken, run on an SDS-PAGE gel and exposed on a phosphor screen, WT MEF samples treated with only DMSO contained radio-labeled proteins over a wide range of molecular weights (Fig. 2-2A). In contrast, MEF treated with HSL-C12 showed very little ^{35}S-labeling, indicating that HSL-C12 was inducing a block in protein synthesis. Coomassie labeling of the SDS-PAGE gel revealed equal protein loading between lanes (Fig. 2-2B), indicating that the difference in radio-labeling was not caused by differential loading. These results suggested that the decoupling of KC gene expression and protein secretion in MEF caused by HSL-C12 was the result of a global reduction in protein synthesis.
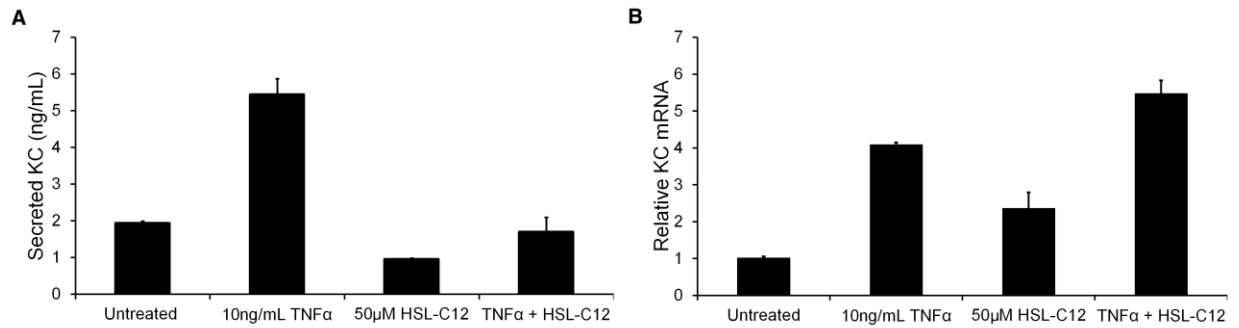
Figure 2-1. Effects of HSL-C12 and TNFα on KC secretion and gene expression. (**A**) KC ELISA. WT MEF were rinsed with fresh media then treated for 4 hours with TNFα, HSL-C12 or TNFα+HSL-C12, and samples were taken from cell medium. Averages +/- Std. Error. (**B**) Quantitative PCR. RNA was isolated from cells in (A), and cDNA was formed for qPCR assay. Results are given as RQ score normalized to RPS17 cDNA. Averages displayed with min and max. N=3 biological replicates for all conditions.
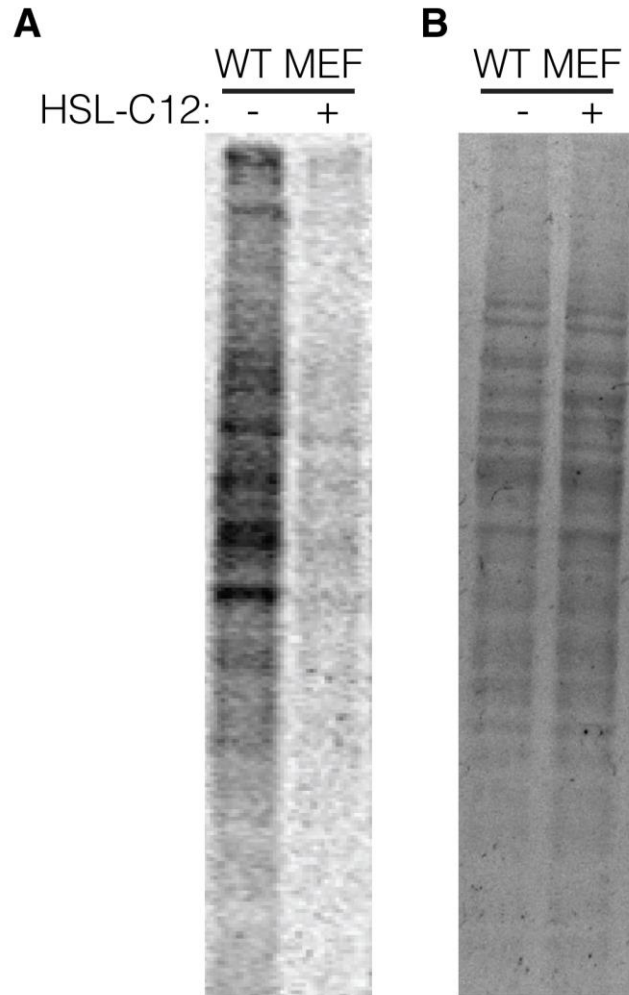
Figure 2-2. Effects of HSL-C12 on protein synthesis. (**A**) ^{35}S methionine radio-labeling of bulk protein from 50μM HSL-C12 or DMSO mock-treated WT MEF imaged with a phosphor screen. HSL-C12 treatments were for 4 hours total with radio-labeling performed during final hour. (**B**) Coomassie-stained SDS-PAGE gel from same experiment. Results are representative of two experiments.

ER Stress Transducer PERK Plays a Role in HSL-C12-Mediated Translation Inhibition

HSL-C12 has previously been shown to induce the phosphorylation of eI-F2α (Kravchenko *et al.*, 2006), and given the known effects of HSL-C12 on the ER (Shiner *et al.*, 2006, Schwarzer *et al.*, 2010, Schwarzer *et al.*, 2012) we explored the role of ER stress transducers in HSL-C12-mediated translation inhibition. The kinase PERK is well established to induce translation-inhibition in response to ER stress by phosphorylating the initiation factor eI-F2α (Harding *et al.*, 1999). To assay the role of PERK in HSL-C12-mediated inhibition of translation, we compared HSL-C12-induced responses in PERK^{-/-} and corresponding PERK-corrected PERK^{-/-} (PERK-corrected) MEF cell lines. Western blot analysis indicated that PERK levels were similar in the WT and PERK-corrected PERK^{-/-} MEF and PERK was absent in PERK^{-/-} MEF (Fig. 2-3A,B). WT and PERK-corrected PERK^{-/-} MEF also displayed a similar gel shift when treated with HSL-C12, consistent with phosphorylation and activation of PERK (Fig. 2-3C). We tested the functional PERK activity of these cell lines by activating ER stress using the common ER stress inducer thapsigargin (Christensen *et al.*, 1993, Harding *et al.*, 1999). There was only a small increase in eI-F2α phosphorylation in PERK^{-/-} cells, while PERK-corrected cells displayed much more phosphorylation as measured in western blots (Fig. 2-3D). Similarly, HSL-C12 increased eI-F2α phosphorylation in PERK-corrected cells compared to PERK^{-/-} cells, particularly during the first two hours of treatment (Fig. 2-4). Finally, when cells were treated with both HSL-C12 and TNFα, there was greater inhibition of protein synthesis in PERK-corrected than PERK^{-/-} cells as measured by ^{35}S labeling (Fig. 2-5). Similar results were obtained with HSL-C12 treatment alone (data not shown). Together these results indicated that a portion of HSL-C12's inhibitory effects on protein synthesis resulted from activation of PERK and the phosphorylation of eI-F2α.
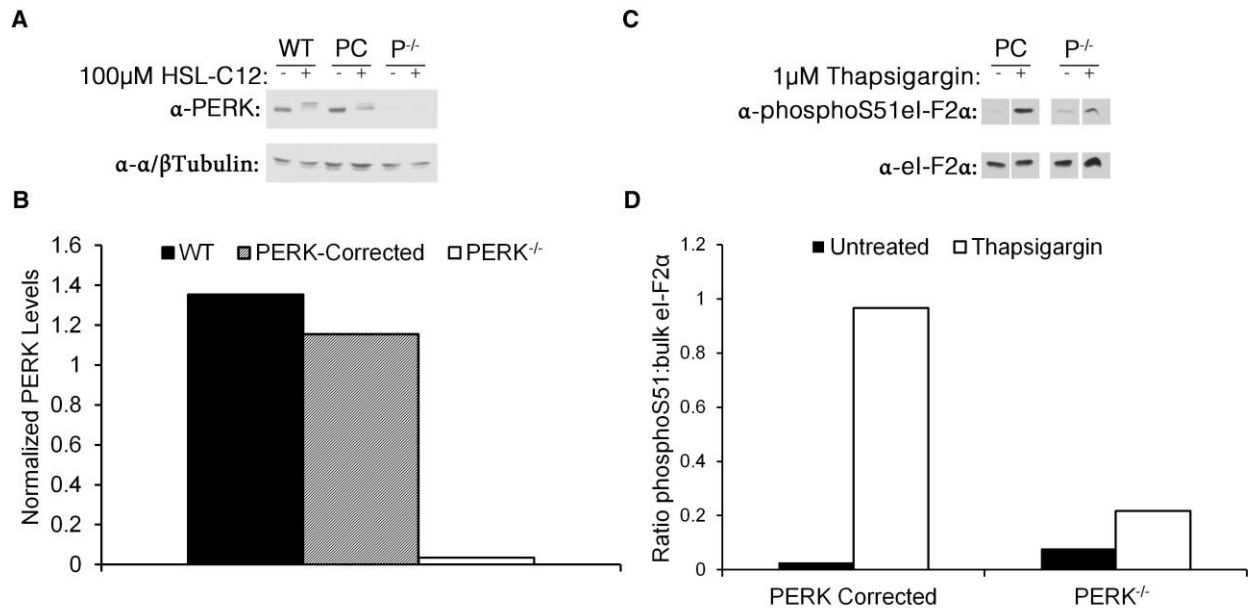
Figure 2-3. WT and PERK-corrected PERK$^{-/-}$ MEF have similar PERK levels. (**A**) WT, PERK-corrected PERK$^{-/-}$ (PC), and PERK$^{-/-}$ (P$^{-/-}$) MEF were either untreated or treated for 1 hour with 100µM HSL-C12. Protein samples were taken, run at equal concentrations on an SDS-PAGE gel, and western blots were performed using anti-PERK and anti-α/βTubulin antibodies. (**B**) Results from untreated lanes from (A) quantified and displayed as ratio PERK to α/βTubulin. Results typical of two experiments. (**C**) PERK-corrected PERK$^{-/-}$ (PC) and PERK$^{-/-}$ (P$^{-/-}$) MEF's were either untreated or treated for 1 hour with 1µM thapsigargin to activate ER stress. Protein samples were taken, run at equal concentrations on an SDS-PAGE gel, and western blots were performed using anti-phosphoS51-eI-F2α and anti-eI-F2α antibodies. (**D**) Results from (C) quantified and displayed as ratio phosphoS51-eI-F2α to bulk eI-F2α. Results typical of two experiments.
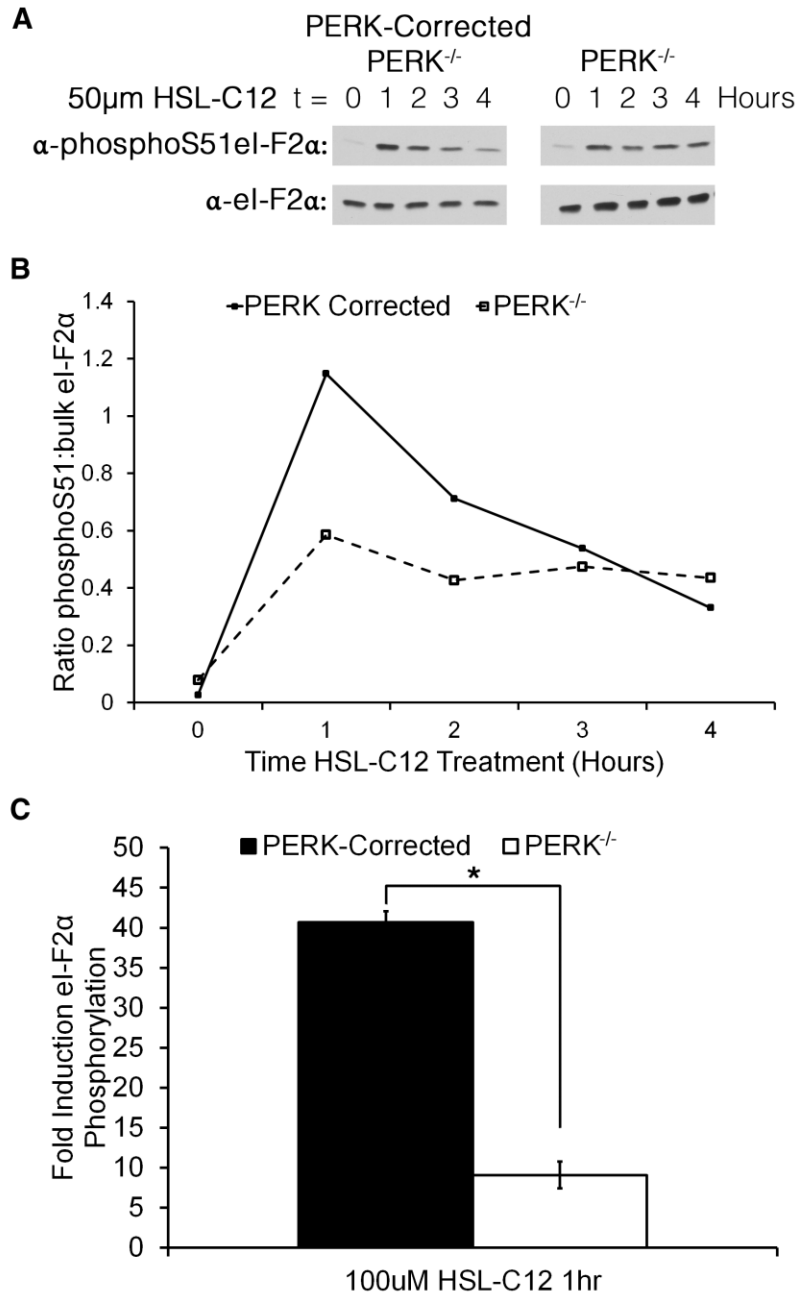
Figure 2-4. Effects of HSL-C12 on elF2α phosphorylation. PERK^{-/-} and PERK-corrected MEF were treated with 50μM HSL-C12 for 0, 1, 2, 3 or 4 hours. (**A**) Protein samples were taken, and run at equal concentrations on an SDS-PAGE gel; western blots were performed using anti-phosphoS51-eI-F2α and anti-eI-F2α antibodies. (**B**) Results from (A) were quantified and displayed as the ratio of phosphoS51-eI-F2α to bulk eI-F2α. (**C**) Average induction of eI-F2α phosphorylation (treated divided by untreated) in response to 1hr 100uM HSL-C12 from western blots. N=2 biological replicates, error bars indicate std. error. *p = 0.00463 in unpaired 2-tailed T-test.
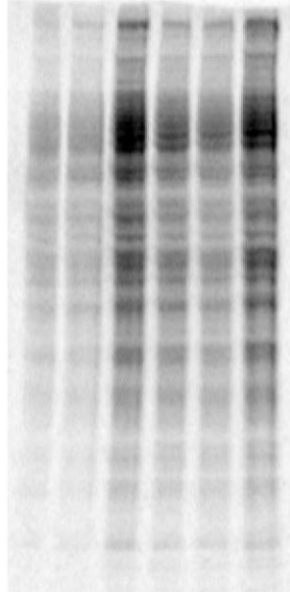
Figure 2-5. HSL-C12 protein synthesis block is PERK-dependent. (**A**) ^{35}S methionine radio-labeling of bulk protein from PERK^{-/-} and PERK-corrected MEF's untreated or treated with 100uM HSL-C12 combined with 10ng/mL TNFα imaged with a phosphor screen. Treatments were for 4 or 8 hours total with radio-labeling performed during final hour. (**B**) Coomassie-stained SDS-PAGE gel from same experiment. (**C**) Graph of phosphor image from (A) quantified and normalized to coomassie image from (B).
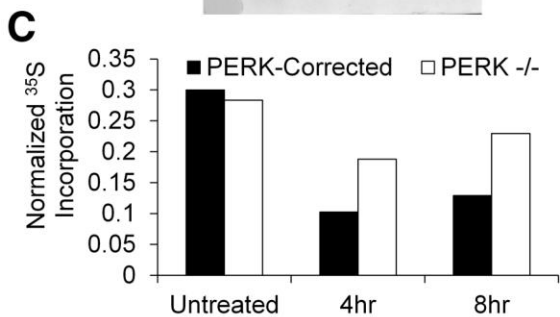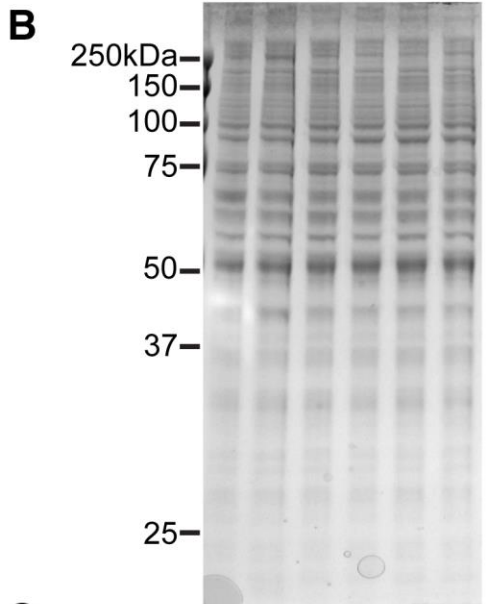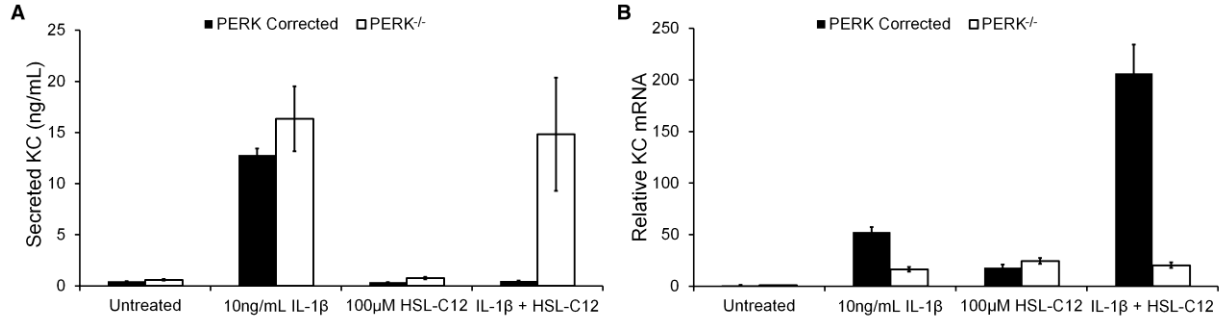
HSL-C12's Effects on KC Expression and Secretion in MEF's are PERK-dependent

The data to this point suggested that HSL-C12 caused a PERK-dependent block in host translation that inhibited the production of the inflammatory cytokine KC. Therefore, we explored PERK's role in the KC responses observed during HSL-C12 treatment. Similar to WT MEF, PERK-corrected MEF secreted very little KC when co-treated with both IL-1β (utilized here because it is a more potent activator of the NF-κB pathway than TNFα in MEF) and HSL-C12 for 4 hours (Fig. 2-6A). Conversely, when co-treated with IL-1β and HSL-C12, PERK$^{-/}$ MEF displayed KC secretion levels similar to IL-1β treatment alone after 4 hours. These data indicated that the HSL-C12-induced block of protein synthesis that is responsible for the reduction in cytokine secretion by MEF was dependent on the kinase PERK and the phosphorylation of eIF2a.

HSL-C12 treatment increased cytokine gene expression so we tested PERK's role in this induction. After 4 hours of IL-1β and HSL-C12 co-treatment, PERK-corrected MEF exhibited higher levels of KC gene expression than cells treated with IL-1β alone (Fig. 2-6B), similar to the effects on WT MEF. Interestingly, PERK$^{-/-}$ MEF showed similar levels of KC gene expression during IL-1β treatment either in the absence or presence of HSL-C12. HSL-C12 on its own did increase KC gene expression in PERK$^{-/-}$ MEF, possibly through another effector pathway, but unlike the PERK-corrected MEF, this effect was not synergistic when combined with IL-1β.

The synergy between IL-1β and HSL-C12 in PERK-corrected MEF's may be explained by the inhibition of protein synthesis. IκB, the repressor of NF-κB, is a high-turnover protein (Krappmann *et al.*, 1997). Treatment with an activator of the NF-κB pathway causes phosphorylation of IκB and increased degradation. It has been reported that activators of PERK, including UV-light, can lead to NF-κB signaling by inhibiting protein synthesis, thereby decreasing the available pool of IκB (Wu *et al.*, 2004). We measured IκBα and p65 (a subunit of NF-κB) levels and found that over the course of 4 hours, HSL-C12 caused IκBα levels to decrease more in PERK-corrected than PERK$^{-/-}$ cells, particularly during the first two hours of treatment (Fig. 2-7A). Levels of p65 were similar between the two lines, so the ratio of p65 to IκB, and therefore potential NF-κB activity, was greater in PERK-corrected cells during the first two hours of treatment. These results indicated that PERK was responsible for a major part of both the anti-secretion and also the pro-gene expression effects of HSL-C12 on cytokines. By inhibiting protein synthesis, PERK may have prevented the production and secretion of KC, while synergistically increasing KC gene expression when co-treated with IL-1β by causing reduced re-synthesis of the NF-κB repressor, IκB.

Given the apparent role for PERK in HSL-C12 inflammatory phenotypes, we also tested whether PERK might play a role in other HSL-C12-triggered responses. PERK and other members of the unfolded protein response are known to produce pro-apoptotic signals under certain conditions (Jordan *et al.*, 2002, Oyadomari *et al.*, 2002). However, caspase 3/7 activation assays did not reveal any differences between PERK-corrected and PERK$^{-/-}$ cells treated with HSL-C12 (Fig. 2-8). HSL-C12 has also been reported to cause depolarization of mitochondrial membrane potential (Schwarzer *et al.*, 2012), but PERK-corrected and PERK$^{-/-}$ cells showed similar HSL-C12-induced rates of depolarization of mitochondrial membrane potential as measured using the dye JC-1 (data not shown). Together these results indicated that HSL-C12 affected KC signaling and apoptosis through different pathways.

Figure 2-6. HSL-C12 effects on KC secretion and gene expression are PERK-dependent.
(**A**) KC ELISA. PERK^{-/-} and PERK-corrected MEF were rinsed with fresh media then treated for 4 hours with TNFα, HSL-C12 or TNFα+HSL-C12, and samples were taken from cell medium. Averages +/- Std. Error. (**B**) Quantitative PCR. RNA was isolated from cells in (A), and cDNA was formed for qPCR assay. Results are given as RQ score normalized to RPS17 cDNA. Averages displayed with min and max. N=3 biological replicates for all conditions.

A

PERK-Corrected

PERK$^{-/-}$ PERK$^{-/-}$

100µm HSL-C12 t = 0 1 2 3 4   0 1 2 3 4 Hours

α-IκBα:

α-p65:

B
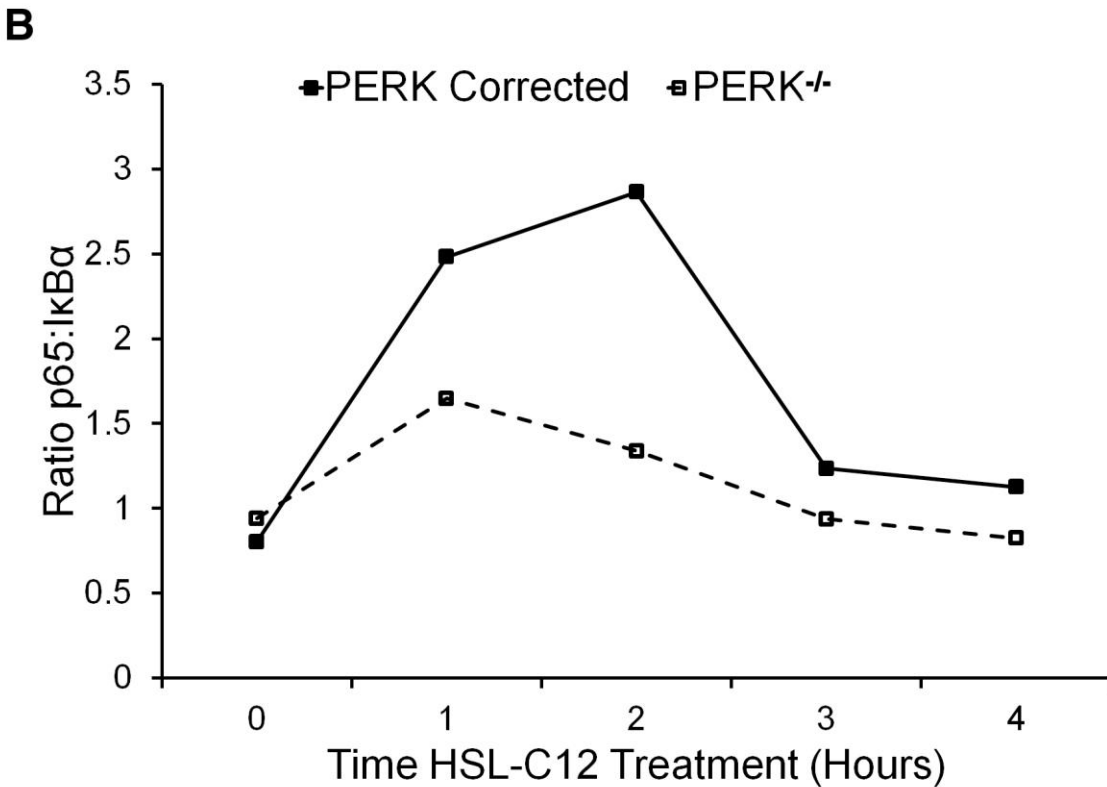
Figure 2-7. HSL-C12-induced degradation of IκBα is PERK-dependent. PERK$^{-/-}$ and PERK-corrected MEF were treated with 100µM HSL-C12. (**A**) Protein samples were taken from cells at times shown, and run at equal concentrations on an SDS-PAGE gel; western blots were performed using anti-IκBα and anti-p65 antibodies. (**B**) Results from (A) quantified and displayed as ratio p65 to bulk IκBα. High ratios indicate high potential for NF-κB p65 driven transcription. Results typical of two experiments.
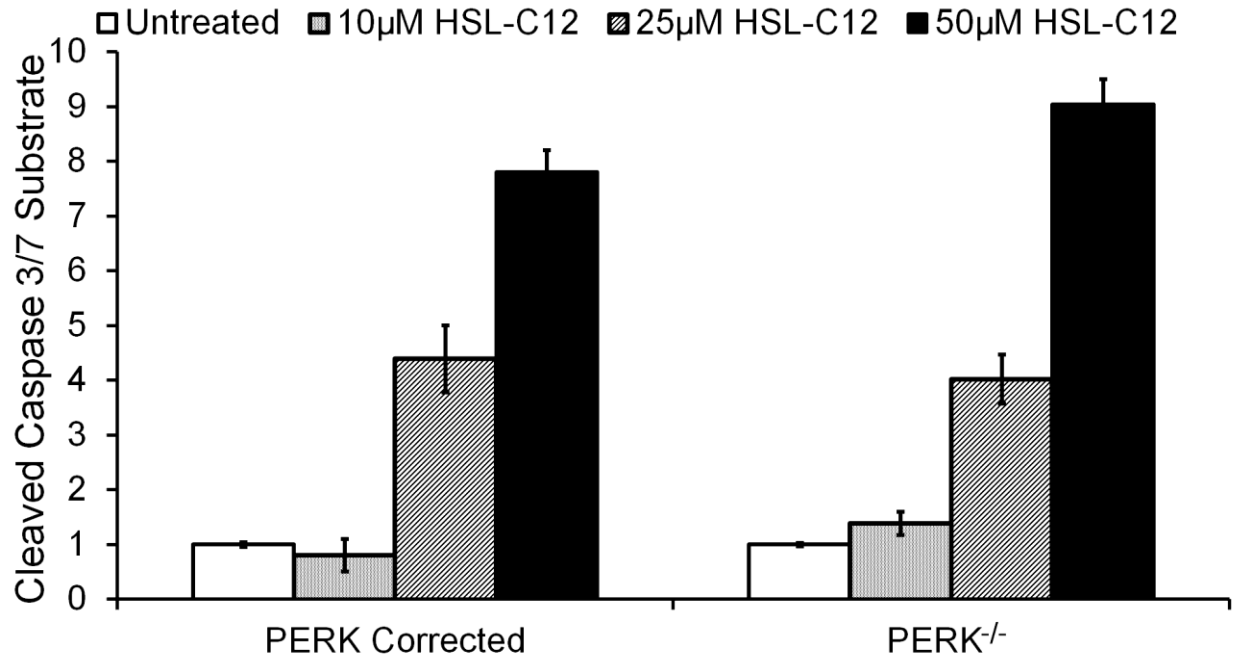
Figure 2-8. HSL-C12 induced apoptosis is PERK-independent. PERK$^{-/-}$ and PERK-corrected MEF's were treated with increasing doses of HSL-C12, and caspase 3/7 activation was measured. N=3 biological replicates, averages with std. error plotted.

HSL-C12-mediated Block of KC Secretion is Temporary

It has been reported that HSL-C12's effects vary based on the length of exposure (Vikström *et al.*, 2006). We therefore compared HSL-C12's effects on TNFα-induced KC secretion and gene expression during 4 and 8 hour treatments. At 4 hours, HSL-C12 inhibited TNFα-induced KC secretion and increased TNFα-induced KC gene expression in PERK-corrected cells (Fig. 2-9). However, at 8 hours, HSL-C12 caused an increase in TNFα-induced KC secretion but only minimally increased KC expression, especially compared to the effects at 4 hours, in PERK-corrected cells. This transition from suppression to induction of cytokine protein was confirmed in WT MEF using an NF-κB-driven luciferase assay (Fig. 2-10). This assay was not performed in PERK-corrected or PERK$^{-/-}$ MEF due to reduced transfection efficiencies. There were no apparent effects of HSL-C12 on TNFα-induced KC gene expression or secretion in PERK$^{-/-}$ MEF at either four or eight hours.
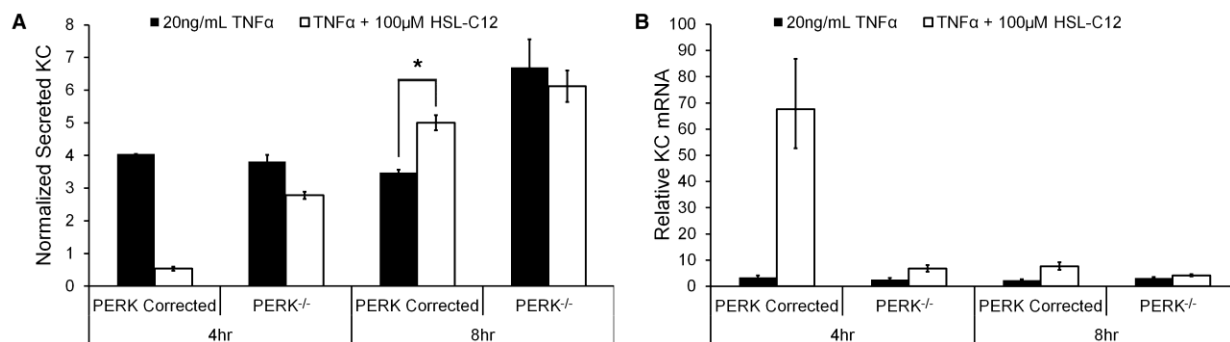
Figure 2-9. Effects of HSL-C12 and TNFα on KC secretion and gene expression at 4 and 8 hrs. (**A**) KC ELISA. PERK^{-/-} and PERK-corrected MEF's were rinsed with fresh medium and then treated for 4 and 8 hours with the indicated treatments, and samples were taken from cell medium. To account for cell death, results were normalized to adherent protein collected from trizol preparation as measured via protein dot blot (data not shown). Averages +/- Std. Error. (**B**) Quantitative PCR. RNA was isolated from cells in (A), and cDNA was formed for qPCR assay. Results are given as RQ score normalized to RPS17 cDNA. Averages displayed with min and max. N=3 biological replicates for all conditions. *p = 0.0337 in unpaired 2-tailed T-test.
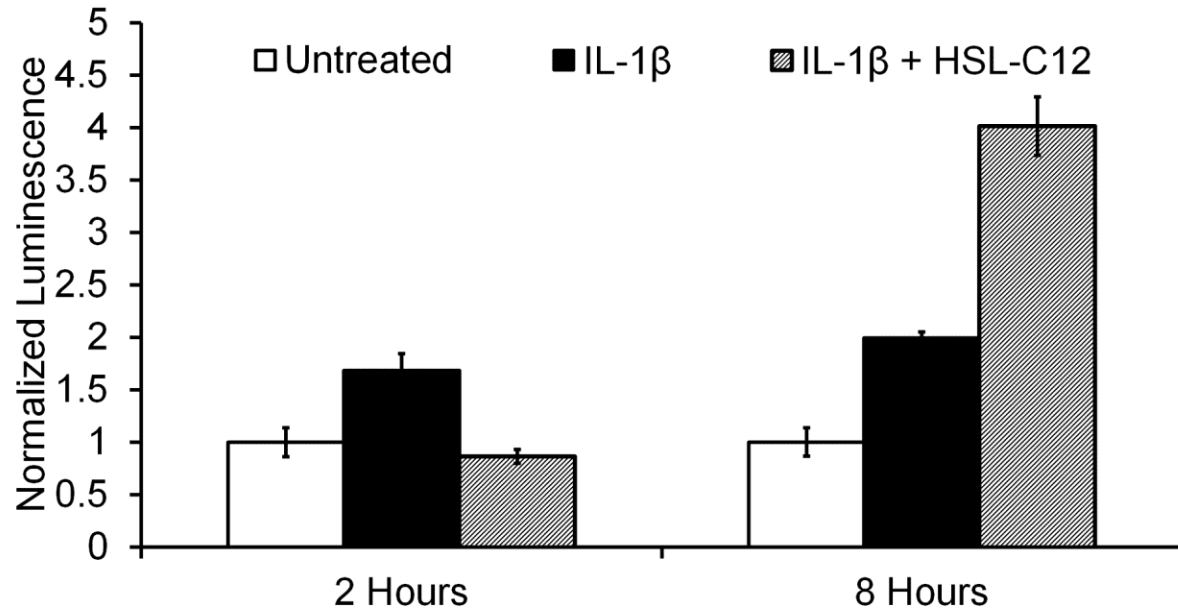
Figure 2-10. HSL-C12 reduces NF-κB luciferase at 2 hours and increases at 8 hours. WT MEF were transfected with a luciferase reporter plasmid utilizing the NF-κB responsive promoter from the ELAM gene. Cells were either untreated, treated with 10ng/mL IL-1β or a combination of IL-1β and 100uM HSL-C12. Cells were harvested after 2 or 8 hours of treatment and samples were analyzed for protein concentration and luciferase activity. Luciferase activity normalized to protein concentration and then to the untreated condition for each time point is plotted. N=4 biological replicates, averages with std. error plotted.
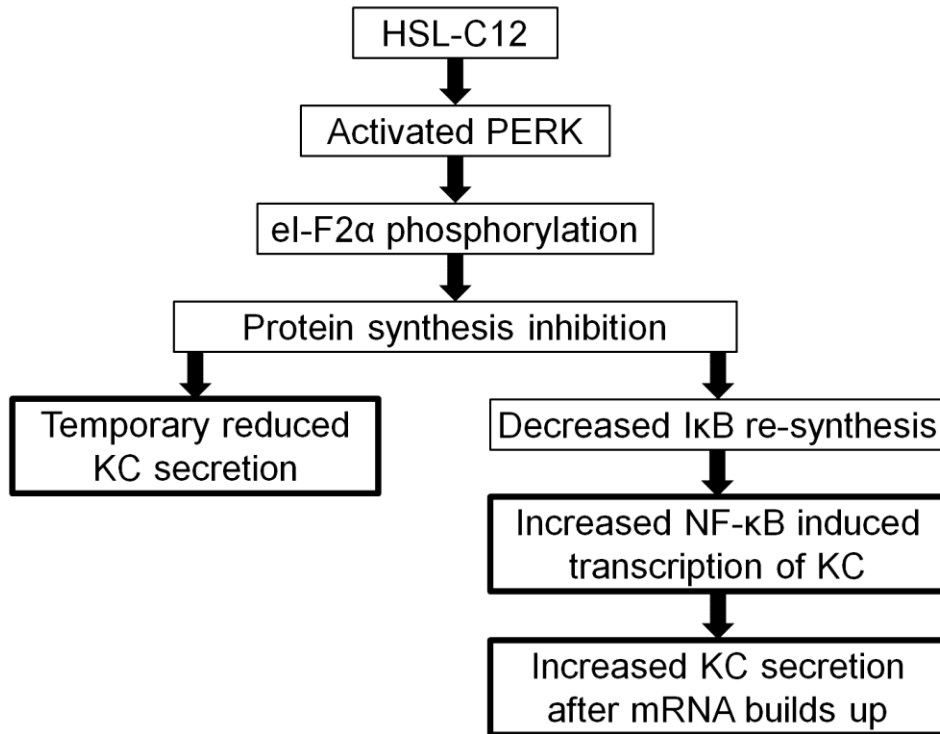
Figure 2-11. Flowchart showing the inflammatory phenotypes observed during HSL-C12 treatment. See text for details.

DISCUSSION

In this study we showed that HSL-C12 reduced KC secretion in 4 hour-treatments, but increased KC secretion in 8 hour-treatments in wild type MEF. Both of these effects were greatly reduced in cells that did not express the ER stress mediator PERK. HSL-C12 also caused the phosphorylation of eI-F2α and inhibition of protein synthesis, and again these effects were muted, though not fully ablated, in PERK$^{-/-}$ MEF. These data were consistent with the interpretation that HSL-C12 acts through the effector proteins PERK and eI-F2α to inhibit protein synthesis, leading to decreased cytokine secretion in the short term (4 hrs), and increased cytokine secretion in the long term (8 hrs), particularly in the presence of the pro-inflammatory mediators IL-1β and TNFα.

A flow chart summarizing our conclusions about the effects of HSL-C12 is presented in Fig. 2-11. HSL-C12 causes the activation of PERK and the subsequent phosphorylation of eI-F2α and inhibition of protein synthesis. Since HSL-C12 causes the release of calcium stores from the ER, and many of the ER chaperones require calcium, it is possible that reducing calcium levels in the ER activates the unfolded protein response and PERK (Christensen *et al.*, 1993, Harding *et al.*, 1999). This is supported by the similarity between responses to HSL-C12 and thapsigargin in PERK$^{-/-}$ and PERK-corrected MEF (Figs. 2-3, 2-4). Once eI-F2α is phosphorylated, new inflammatory protein production will likely be reduced, leading to low levels of secreted cytokines, even in the presence of ligands like TNFα and IL-1β that normally induce inflammatory secretion. However, phosphorylation of eI-F2α also prevents the re-synthesis of IκB, the NF-κB inhibitor. IκB is a high turnover protein (Krappmann *et al.*, 1997), and as IκB levels fall, NF-κB can enter the nucleus and induce transcription of inflammatory gene products. Though HSL-C12-induced protein synthesis inhibition persists up to 8 hours (Fig. 4), HSL-C12 increases TNFα-induced KC secretion by 8 hours (Fig. 7), perhaps because the large amount of KC mRNA produced at 4 hours (Fig. 5) is sufficient to induce increased KC translation and secretion even under conditions of reduced translation. Though protein synthesis is still inhibited in these cells, it does still occur and therefore high transcript levels could lead to preferential translation.

The present work also suggests that HSL-C12 acts through multiple effector pathways in mammalian cells. For example, we observed that PERK was not required for HSL-C12 to activate caspase 3/7 or depolarize the mitochondrial membrane potential. The presence of some eI-F2α phosphorylation and the partial inhibition of protein synthesis observed in PERK$^{-/-}$ cells treated with HSL-C12 was likely the result of another of HSL-C12's effector pathways. One potential candidate is the eI-F2α kinase GCN2, which is activated by metabolic stress through the buildup of unloaded tRNAs (Harding *et al.*, 2003). HSL-C12's effects on the mitochondria (Kravchenko *et al.*, 2006, Schwarzer *et al.*, 2012) may lead to metabolic stress and subsequent GCN2 activation.

Although it has not been fully established that HSL-C12 is an important virulence factor for *P. aeruginosa in vivo*, the present results help to paint a picture of how HSL-C12's effects on inflammatory signaling could affect the course of *P. aeruginosa* infection. HSL-C12 secreted by *P. aeruginosa* would have the short term effects of creating gaps in epithelia resulting from its proapoptotic effects (Tateda *et al.*, 2003, Li *et al.*, 2004b, Jacobi *et al.*, 2009, Schwarzer *et al.*, 2012), while suppressing immune signaling. This would allow *P. aeruginosa* access to the

basolateral membrane, an important factor for virulence (Hybiske *et al.*, 2004), while avoiding immune detection. However, in the long term, HSL-C12 may increase cytokine secretion and contribute to the hyperinflammatory state observed in CF patients infected with *P. aeruginosa*. PERK's role in this effect also suggests ties to phenotypes observed in cells from CF patients. CF airway cells are characterized by increased ER volume and a chronically active unfolded protein response (Martino *et al.*, 2009), perhaps indicating prolonged exposure to ER stress inducers like HSL-C12. This study suggest that HSL-C12 may be an important factor in *P. aeruginosa* infections, and it deserves further study.

CONCLUSIONS

Cystic Fibrosis is the most prevalent genetic disorder among Caucasians and *Pseudomonas aeruginosa* infections represent a clinically significant problem for sufferers of CF (Hoiby *et al.*, 1977). Existing treatments for CF are costly and fail to fully address the issues stemming from the disease. As CF appears to be in part a disease of hyperinflammation, the study of the inflammatory responses to *P. aeruginosa* remains an important field. This study is complicated by the various secreted factors from *P. aeruginosa* which affect immune secretion and signaling. The present study highlights the complicated nature of the mammalian response to *P. aeruginosa* factors. The data acquired from flagellin-induced chloride secretion paint a picture of multiple signaling pathways affecting secretion through the CFTR, and perhaps through tight junctions as well. The data acquired on HSL-C12's effects on cytokine secretion show a bi-phasic response mediated by multiple effector pathways as well, though my data suggest that the ER stress transducer PERK is mostly responsible for HSL-C12'short term anti-inflammatory and long term pro-inflammatory effects. There remain multiple questions to be answered in both of these systems. It is still unclear which receptor is mediating flagellin-induced chloride currents and what the primary intracellular effector molecules are. It is also unclear which receptor is mediating HSL-C12 responses and if PERK's role in HSL-C12 responses is an effect of the canonical UPR pathway observed when cells are treated with thapsigargin or tunicamycin or a novel use of PERK. Lastly, it remains to be seen if *P. aeruginosa* biolfilms will have a similar effect on inflammatory signaling as purified HSL-C12 and if the PERK-mediated response exists in other cell types and is an important factor is *P. aeruginosa* infections. The present study shows that the study of *P. aeruginosa* secreted factor holds promise for understanding *P. aeruginosa* infections in CF, but much work remains to be done and there are many gaps left to bridge.

REFERENCES

Adamo, R., Sokol, S., Soong, G., Gomez, M.I. and Prince, A. (2004). Pseudomonas aeruginosa flagella activate airway epithelial cells through asialoGM1 and toll-like receptor 2 as well as toll-like receptor 5. *American journal of respiratory cell and molecular biology* **30,** 627-634.

Bear, C.E., Li, C., Kartner, N., Bridges, R.J., Jensen, T.J., Ramjeesingh, M. and Riordan, J.R. (1992). Purification and functional reconstitution of the cystic fibrosis transmembrane conductance regulator (CFTR). *Cell* **68,** 809-818.

Becq, F., Jensen, T.J., Chang, X.-B., Savoia, A., Rommens, J.M., Tsui, L.-C.*, et al.* (1994). Phosphatase inhibitors activate normal and defective CFTR chloride channels. *Proceedings of the National Academy of Sciences* **91,** 9160-9164.

Benali, R., Pierrot, D., Zahm, J.M., de Bentzmann, S. and Puchelle, E. (1994). Effect of extracellular ATP and UTP on fluid transport by human nasal epithelial cells in culture. *American Journal of Respiratory Cell and Molecular Biology* **10,** 363-368.

Bertolotti, A., Zhang, Y., Hendershot, L.M., Harding, H.P. and Ron, D. (2000). Dynamic interaction of BiP and ER stress transducers in the unfolded-protein response. *Nat Cell Biol* **2,** 326-332.

Cain, R.J., Vanhaesebroeck, B. and Ridley, A.J. (2010). The PI3K p110α isoform regulates endothelial adherens junctions via Pyk2 and Rac1. *The Journal of cell biology* **188,** 863-876.

Cheng, S.H., Rich, D.P., Marshall, J., Gregory, R.J., Welsh, M.J. and Smith, A.E. (1991). Phosphorylation of the R domain by cAMP-dependent protein kinase regulates the CFTR chloride channel. *Cell* **66,** 1027-1036.

Choi, Y.J., Im, E., Chung, H.K., Pothoulakis, C. and Rhee, S.H. (2010). TRIF mediates Toll-like receptor 5-induced signaling in intestinal epithelial cells. *Journal of Biological Chemistry* **285,** 37570-37578.

Christensen, S.B., Andersen, A., Poulsen, J.-C.J. and Treiman, M. (1993). Derivatives of thapsigargin as probes of its binding site on endoplasmic reticulum Ca2+ ATPase: Stereoselectivity and important functional groups. *FEBS Letters* **335,** 345-348.

Dupont, G., Combettes, L., Bird, G.S. and Putney, J.W. (2011). Calcium Oscillations. *Cold Spring Harbor Perspectives in Biology* **3**.

French, P.J., Bijman, J., Edixhoven, M., Vaandrager, A.B., Scholte, B.J., Lohmann, S.M.*, et al.* (1995). Isotype-specific activation of cystic fibrosis transmembrane conductance regulator-chloride channels by cGMP-dependent protein kinase II. *Journal of Biological Chemistry* **270,** 26626-26631.

Fu, Z., Bettega, K., Carroll, S., Buchholz, K.R. and Machen, T.E. (2007). Role of Ca2+ in responses of airway epithelia to Pseudomonas aeruginosa, flagellin, ATP, and thapsigargin. *American Journal of Physiology-Lung Cellular and Molecular Physiology* **292,** L353-L364.

Gadsby, D.C. and Nairn, A.C. (1999). Control of CFTR channel gating by phosphorylation and nucleotide hydrolysis. *Physiological reviews* **79,** S77-S107.

Gadsby, D.C., Vergani, P. and Csanády, L. (2006). The ABC protein turned chloride channel whose failure causes cystic fibrosis. *Nature* **440,** 477-483.

Hanoune, J. and Defer, N. (2001). Regulation and role of adenylyl cyclase isoforms. *Annual review of pharmacology and toxicology* **41,** 145-174.

Hanrahan, J.W., Zhu, T. and Howell, L.D. (2003). Phosphatase Regulation of CFTR. *The Cystic Fibrosis Transmembrane Conductance Regulator*, 35.

Harding, H.P., Zhang, Y. and Ron, D. (1999). Protein translation and folding are coupled by an endoplasmic-reticulum-resident kinase. *Nature* **397,** 271-274.

Harding, H.P., Zhang, Y., Zeng, H., Novoa, I., Lu, P.D., Calfon, M*., et al.* (2003). An Integrated Stress Response Regulates Amino Acid Metabolism and Resistance to Oxidative Stress. *Molecular Cell* **11,** 619-633.

Hayashi, F., Smith, K.D., Ozinsky, A., Hawn, T.R., Yi, E.C., Goodlett, D.R*., et al.* (2001). The innate immune response to bacterial flagellin is mediated by Toll-like receptor 5. *Nature* **410,** 1099-1103.

Hinnebusch, A.G. (1994) The eIF-2α kinases: regulators of protein synthesis in starvation and stress. In *Seminars in cell biology*. Elsevier, pp. 417-426.

Hoiby, N., Flensborg, E.W., Beck, B., Friis, B., Jacobsen, S.V. and Jacobsen, L. (1977). Pseudomonas aeruginosa infection in cystic fibrosis. Diagnostic and prognostic significance of Pseudomonas aeruginosa precipitins determined by means of crossed immunoelectrophoresis. *Scandinavian journal of respiratory diseases* **58,** 65-79.

Hybiske, K., Ichikawa, J.K., Huang, V., Lory, S.J. and Machen, T.E. (2004). Cystic fibrosis airway epithelial cell polarity and bacterial flagellin determine host response to Pseudomonas aeruginosa. *Cellular microbiology* **6,** 49-63.

Idzko, M., Hammad, H., van Nimwegen, M., Kool, M., Willart, M.A.M., Muskens, F*., et al.* (2007). Extracellular ATP triggers and maintains asthmatic airway inflammation by activating dendritic cells. *Nat Med* **13,** 913-919.

Illek, B., Fu, Z., Schwarzer, C., Banzon, T., Jalickee, S., Miller, S.S. and Machen, T.E. (2008). Flagellin-stimulated Cl− secretion and innate immune responses in airway epithelia: role for p38. *American Journal of Physiology-Lung Cellular and Molecular Physiology* **295,** L531-L542.

Irie, Y. and Parsek, M. (2008) Quorum sensing and microbial biofilms. In *Bacterial biofilms*. Springer, pp. 67-84.

Jacobi, C.A., Schiffner, F., Henkel, M., Waibel, M., Stork, B., Daubrawa, M*., et al.* (2009). Effects of bacterial< i> N</i>-acyl homoserine lactones on human Jurkat T lymphocytes-OdDHL induces apoptosis via the mitochondrial pathway. *International Journal of Medical Microbiology* **299,** 509-519.

Jahoor, A., Patel, R., Bryan, A., Do, C., Krier, J., Watters, C*., et al.* (2008). Peroxisome proliferator-activated receptors mediate host cell proinflammatory responses to Pseudomonas aeruginosa autoinducer. *Journal of bacteriology* **190,** 4408-4415.

Jordan, R., Wang, L., Graczyk, T.M., Block, T.M. and Romano, P.R. (2002). Replication of a cytopathic strain of bovine viral diarrhea virus activates PERK and induces endoplasmic reticulum stress-mediated apoptosis of MDBK cells. *Journal of virology* **76,** 9588-9599.

Kaufman, R.J. (1999). Stress signaling from the lumen of the endoplasmic reticulum: coordination of gene transcriptional and translational controls. *Genes & Development* **13,** 1211-1233.

Krappmann, D. and Scheidereit, C. (1997). Regulation of NF-κB activity by IκBα and IκBβ stability. *Immunobiology* **198,** 3-13.

Kravchenko, V.V., Kaufmann, G.F., Mathison, J.C., Scott, D.A., Katz, A.Z., Grauer, D.C*., et al.* (2008). Modulation of gene expression via disruption of NF-κB signaling by a bacterial small molecule. *Science* **321,** 259-263.

Kravchenko, V.V., Kaufmann, G.F., Mathison, J.C., Scott, D.A., Katz, A.Z., Wood, M.R.*, et al.* (2006). N-(3-oxo-acyl) homoserine lactones signal cell activation through a mechanism distinct from the canonical pathogen-associated molecular pattern recognition receptor pathways. *Journal of Biological Chemistry* **281,** 28822-28830.

Kulaksiz, H., Schmid, A., Hönscheid, M., Ramaswamy, A. and Cetin, Y. (2002). Clara cell impact in air-side activation of CFTR in small pulmonary airways. *Proceedings of the National Academy of Sciences* **99,** 6796-6801.

Lefkimmiatis, K., Srikanthan, M., Maiellaro, I., Moyer, M.P., Curci, S. and Hofer, A.M. (2009). Store-operated cyclic AMP signalling mediated by STIM1. *Nature cell biology* **11,** 433-442.

Li, H., Sheppard, D.N. and Hug, M.J. (2004a). Transepithelial electrical measurements with the Ussing chamber. *Journal of Cystic Fibrosis* **3,** 123-126.

Li, H., Wang, L., Ye, L., Mao, Y., Xie, X., Xia, C.*, et al.* (2009). Influence of Pseudomonas aeruginosa quorum sensing signal molecule N-(3-oxododecanoyl) homoserine lactone on mast cells. *Medical microbiology and immunology* **198,** 113-121.

Li, L., Hooi, D., Chhabra, S.R., Pritchard, D. and Shaw, P.E. (2004b). Bacterial N-acylhomoserine lactone-induced apoptosis in breast carcinoma cells correlated with down-modulation of STAT3. *Oncogene* **23,** 4894-4902.

Liedtke, C.M. and Cole, T.S. (1998). Antisense oligonucleotide to PKC-ε alters cAMP-dependent stimulation of CFTR in Calu-3 cells. *American Journal of Physiology-Cell Physiology* **275,** C1357-C1364.

Martino, M.E., Olsen, J.C., Fulcher, N.B., Wolfgang, M.C., O'Neal, W.K. and Ribeiro, C.M. (2009). Airway epithelial inflammation-induced endoplasmic reticulum Ca2+ store expansion is mediated by X-box binding protein-1. *Journal of Biological Chemistry* **284,** 14904-14913.

McNamara, N., Gallup, M., Sucher, A., Maltseva, I., McKemy, D. and Basbaum, C. (2006). AsialoGM1 and TLR5 cooperate in flagellin-induced nucleotide signaling to activate Erk1/2. *American journal of respiratory cell and molecular biology* **34,** 653.

McNamara, N., Khong, A., McKemy, D., Caterina, M., Boyer, J., Julius, D. and Basbaum, C. (2001). ATP transduces signals from ASGM1, a glycolipid that functions as a bacterial receptor. *Proceedings of the National Academy of Sciences* **98,** 9086-9091.

Naren, A.P., Cobb, B., Li, C., Roy, K., Nelson, D., Heda, G.D.*, et al.* (2003). A macromolecular complex of β2 adrenergic receptor, CFTR, and ezrin/radixin/moesin-binding phosphoprotein 50 is regulated by PKA. *Proceedings of the National Academy of Sciences* **100,** 342-346.

Ong, H.L., Cheng, K.T., Liu, X., Bandyopadhyay, B.C., Paria, B.C., Soboloff, J.*, et al.* (2007). Dynamic assembly of TRPC1-STIM1-Orai1 ternary complex is involved in store-operated calcium influx Evidence for similarities in store-operated and calcium release-activated calcium channel components. *Journal of Biological Chemistry* **282,** 9105-9116.

Oyadomari, S., Araki, E. and Mori, M. (2002). Endoplasmic reticulum stress-mediated apoptosis in pancreatic β-cells. *Apoptosis* **7,** 335-345.

Rumbaugh, K.P. (2007). Convergence of hormones and autoinducers at the host/pathogen interface. *Analytical and bioanalytical chemistry* **387,** 425-435.

Schuster, M. and Peter Greenberg, E. (2006). A network of networks: Quorum-sensing gene regulation in< i> Pseudomonas aeruginosa</i>. *International journal of medical microbiology* **296,** 73-81.

Schwarzer, C., Fu, Z., Patanwala, M., Hum, L., Lopez-Guzman, M., Illek, B.*, et al.* (2012). Pseudomonas aeruginosa biofilm-associated homoserine lactone C12 rapidly activates apoptosis in airway epithelia. *Cellular microbiology* **14,** 698-709.

Schwarzer, C., Wong, S., Shi, J., Matthes, E., Illek, B., Ianowski, J.P.*, et al.* (2010). Pseudomonas aeruginosa homoserine lactone activates store-operated cAMP and cystic fibrosis transmembrane regulator-dependent Cl− secretion by human airway epithelia. *Journal of Biological Chemistry* **285,** 34850-34863.

Sheth, P., Basuroy, S., Li, C., Naren, A.P. and Rao, R.K. (2003). Role of phosphatidylinositol 3-kinase in oxidative stress-induced disruption of tight junctions. *Journal of Biological Chemistry* **278,** 49239-49245.

Shiner, E., Terentyev, D., Bryan, A., Sennoune, S., Martinez-Zaguilan, R., Li, G.*, et al.* (2006). Pseudomonas aeruginosa autoinducer modulates host cell responses through calcium signalling. *Cellular microbiology* **8,** 1601-1610.

Smith, K.D., Andersen-Nissen, E., Hayashi, F., Strobe, K., Bergman, M.A., Barrett, S.L.R.*, et al.* (2003). Toll-like receptor 5 recognizes a conserved site on flagellin required for protofilament formation and bacterial motility. *Nature immunology* **4,** 1247-1253.

Smith, R.S., Fedyk, E.R., Springer, T., Mukaida, N., Iglewski, B.H. and Phipps, R.P. (2001). IL-8 production in human lung fibroblasts and epithelial cells activated by the Pseudomonas autoinducer N-3-oxododecanoyl homoserine lactone is transcriptionally regulated by NF-κB and activator protein-2. *The Journal of Immunology* **167,** 366-374.

Smith, R.S., Kelly, R., Iglewski, B.H. and Phipps, R.P. (2002). The Pseudomonas autoinducer N-(3-oxododecanoyl) homoserine lactone induces cyclooxygenase-2 and prostaglandin E2 production in human lung fibroblasts: implications for inflammation. *The Journal of Immunology* **169,** 2636-2642.

Sun, F., Hug, M.J., Lewarchik, C.M., Yun, C.-H.C., Bradbury, N.A. and Frizzell, R.A. (2000). E3KARP mediates the association of ezrin and protein kinase A with the cystic fibrosis transmembrane conductance regulator in airway cells. *Journal of Biological Chemistry* **275,** 29539-29546.

Tateda, K., Ishii, Y., Horikawa, M., Matsumoto, T., Miyairi, S., Pechere, J.C.*, et al.* (2003). The Pseudomonas aeruginosa autoinducer N-3-oxododecanoyl homoserine lactone accelerates apoptosis in macrophages and neutrophils. *Infection and immunity* **71,** 5785-5793.

Telford, G., Wheeler, D., Williams, P., Tomkins, P., Appleby, P., Sewell, H.*, et al.* (1998). The Pseudomonas aeruginosaQuorum-Sensing Signal MoleculeN-(3-Oxododecanoyl)-l-Homoserine Lactone Has Immunomodulatory Activity. *Infection and Immunity* **66,** 36-42.

Tuo, B., Wen, G., Song, P., Xu, J., Liu, X., Seidler, U. and Dong, H. (2011). Genistein stimulates duodenal HCO< sub> 3</sub>< sup>−</sup> secretion through PI3K pathway in mice. *European journal of pharmacology* **651,** 159-167.

Tuo, B., Wen, G., Zhang, Y., Liu, X., Wang, X., Liu, X. and Dong, H. (2009). Involvement of phosphatidylinositol 3-kinase in cAMP-and cGMP-induced duodenal epithelial CFTR activation in mice. *American Journal of Physiology-Cell Physiology* **297,** C503-C515.

Vikström, E., Tafazoli, F. and Magnusson, K.-E. (2006). < i> Pseudomonas aeruginosa</i> quorum sensing molecule< i> N</i>-(3 oxododecanoyl)-l-homoserine lactone disrupts epithelial barrier integrity of Caco-2 cells. *FEBS letters* **580,** 6921-6928.

West, A.P., Dancho, B.A. and Mizel, S.B. (2005). Gangliosides inhibit flagellin signaling in the absence of an effect on flagellin binding to toll-like receptor 5. *Journal of Biological Chemistry* **280,** 9482-9488.

Wu, S., Tan, M., Hu, Y., Wang, J.-L., Scheuner, D. and Kaufman, R.J. (2004). Ultraviolet light activates NFκB through translational inhibition of IκBα synthesis. *Journal of Biological Chemistry* **279,** 34898-34902.

Yu, Y., Nagai, S., Wu, H., Neish, A.S., Koyasu, S. and Gewirtz, A.T. (2006). TLR5-mediated phosphoinositide 3-kinase activation negatively regulates flagellin-induced proinflammatory gene expression. *The Journal of Immunology* **176,** 6194-6201.

Zhang, Z., Louboutin, J.-P., Weiner, D.J., Goldberg, J.B. and Wilson, J.M. (2005). Human airway epithelial cells sense Pseudomonas aeruginosa infection via recognition of flagellin by Toll-like receptor 5. *Infection and immunity* **73,** 7151-7160.